Characterising Weak Interactions in Solution.

An NMR Spectroscopic Approach.

SCOTT WILCOX

Abstract

Wilcox, S. 2022. Characterising Weak Interactions in Solution.. An NMR Spectroscopic Approach.. *Digital Comprehensive Summaries of Uppsala Dissertations from the Faculty of Science and Technology* 2184. 72 pp. Uppsala: Acta Universitatis Upsaliensis. ISBN 978-91-513-1584-3.

Detecting and characterising weak interactions in dilute solutions is challenging. This thesis focusses on the development of a new NMR spectroscopic strategy to do so, whilst also investigates a newly proposed type of weak interaction in solution with currently available NMR techniques.

Newly developed lanthanide(III) ion complexes bearing Lewis basic and Lewis acidic functionalities were synthesised, and their paramagnetic properties were successfully exploited. In both instances and in an iterative manner, a series of small molecules of different hydrogen- and halogen-bond strengths were titrated against a paramagnetic Lewis base/acid host in the polar aprotic solvent d-MeCN. In all cases, binding phenomena were detected at 1.82-2.20 mM concentrations of host – around an order of magnitude lower than previously attainable. Titrations against diamagnetic references, with Lu(III) complexes and with untagged Lewis bases, provided small, almost undetectable changes in chemical shift upon binding. Dilutions and titration against non-bonding paramagnetic complexes, as well as with a non-bonding species, proved that the paramagnetic properties were indeed transferred through binding the Lewis base or acid to the respective titrants. Association constants were determined for each binding pair, as well as their relative geometry to one another, providing evidence of these weak interactions over a much lower concentration range than was previously possible. This strategy represents the first use of paramagnetic NMR to study weak, small-molecule interactions in solution, thus opening up a whole new field of research with potential applications as a new method in the supramolecular toolbox.

In this thesis I also disprove the existence of the recently proposed 'nucleophilic iodonium interaction,' a hypothetical force between cationic silver(I) and cationic iodine(I) complexes in solution. Through means of 1H,15N HMBC and DOSY NMR experiments, the lack of interaction between iodine(I) and silver(I) in mixtures of both fast-exchanging bis(pyridine) complexes and slow-exchanging 1,2-bis((pyridine-2-ylethynyl)-benzene) complexes of the two is demonstrated. Testing purposefully contaminated samples of each, separately and in a mixture, lead to the conclusion that the initially published results were anomalous due to wet, consequently decomposed samples. DFT calculations corroborate the experimental findings, suggesting a π-π interactions to be responsible for previously reported crystal structure. These results highlight the need for the careful appraisal of new scientific ideas and the critical interpretation of experimental and computational data.

Scott Wilcox, Department of Chemistry - BMC, Organic Chemistry, Box 576, Uppsala University, SE-75123 Uppsala, Sweden.

Perseverance.
The courage to ignore the obvious wisdom of turning back.

List of Papers

This thesis is based on the following papers, which are referred to in the text by their Roman numerals.

I.   Wilcox, S., Xiong, R., Erdélyi, M. (2022) A new NMR methodology to study weak interactions in solution. *Manuscript.*

II. Berionni Berna, B., Wilcox, S., Xiong, R., Erdélyi, M. (2022) Exceeding the Limits of Characterising Weak Interactions in Dilute Solutions. *Manuscript.*

III. Wilcox, S., Sethio, D., Ward, J. S., Frontera, A., Lindh, R., Rissanen. K., Erdélyi, M. Do 2-coordinate iodine (I) and silver (I) complexes form nucleophilic iodonium interactions (NIIs) in solution? *Chem. Commun.*, **2022**, *58*, 4977-4980

Reprints were made with permission from the respective publishers.

The following publications are not included as part of this thesis:

IV.   Wilcox, S., Herrebout, W. E., Erdélyi, M. Spectroscopy of halogen bonding in solution, in *Halogen Bonding in Solution*, Ed. Huber, S., Wiley VCH, Weinheim, Germany, **2021**, 153-194.

V.   Wieske, L. H. E., Bogaerts, J., Leding, A. A. M., Wilcox S., Andersson Rasmussen, A., Leszczak, K., Turunen, L., Herrebout, W. E., Hubert, M., Bayer, A., Erdélyi, M. NMR Backbone Assignment of VIM-2 and Identification of the Active Enantiomer of a Potential Inhibitor, *ACS Med. Chem. Lett.*, **2022**, *13*, 257-261.

VI.   Solga, D., Zeilinger, C., Herrmann, J., Müller, R., Wilcox, S., Wieske, L. H. E., Erdelyi, M., Kirschning, A. (2022) The oligoarylamide units of cystobactamids are a DNA-binding motif, *Manuscript*.

Contents

Abbreviations

3c4e	3-centred 4-electron (bond)
δ	chemical shift
DEA	diethylamine
DFT	density functional theory
DIPEA	*N,N*-diisopropylethylamine
DMF	dimethylformamide
DOSY	diffusion ordered spectroscopy
DOTA	1,4,7,10-tetraazacyclododecane-1,4,7,10-tetraacetic acid
ESR	electron spin resonance
EXSY	exchange spectroscopy
HB	hydrogen bond(ing)
HMBC	heteronuclear multiple bond correlation (spectroscopy)
HSQC	heteronuclear single quantum coherence (spectroscopy)
IR	infrared
ITC	isothermal titration calorimetry
IUPAC	International Union of Pure and Applied Chemistry
K_a	association constant
kJ	kilojoule
Ln	lanthanide
NII	nucleophilic iodonium interaction
NMR	nuclear magnetic resonance
NOESY	nuclear Overhauser enhancement spectroscopy
PCS	pseudocontact shift
ppm	parts per million
PRE	paramagnetic relaxation enhancement
RDC	residual dipolar coupling
rt	room temperature
TACN	1,4,7-triazacyclononane
TEMPO	2,2,6,6-tetramethyl-1-piperidinyloxy radical
TFA	trifluoroacetic acid
TMS	trimethylsilyl
UV-Vis	ultraviolet-visible (light)
XB	halogen bond(ing)
MW	microwave (irradiation/reactor)
vdW	van der Waals

1. Introduction

Chemical bonds do not actually exist.[1] They are merely a convenient way of explaining complex phenomena that we cannot see nor fully explain, in a way that is most simple, rational and consistent to others.[2] These models have been refined over the years, sometimes conflicting and contradicting one another in the process. Therefore, to gain a clearer and deeper understanding of bonding, so to make better models, we need new, more sensitive methods.

Despite this, we are commonly taught that molecules are held together in two distinct ways, with the dominant attractive forces being intramolecular bonds. These are either more ionic or more covalent in character depending on the differences in electronegativity of their component atoms. Ionic bonds most often possess a large difference between the two, and covalent bonds (and metallic bonds) are more similar in electronegativity. The distinction between them is made at around an electronegativity difference of 2.0, although in reality this ionic/covalent character is better thought of as being on a sliding scale.[3] Pertinent evidence of this is seen in 3-centred N-I-N interactions that possess as much covalent as non-covalent character.[4]

In contrast, intermolecular bonds – the interactions between two molecules – exist as a plethora of weaker interactions (Table 1). The strongest of these are typically hydrogen bonds, followed by various van der Waal's forces, π-interactions and hydrophobic effects. More recently, additional new types of non-covalent interactions, such as halogen, chalcogen,[5] pnictogen and tetrel bonding,[6] and even spectacular cation-cation interactions, such as 'nucleophilic iodonium interactions' have been proposed.[7, 8] Models exist to define these interactions but their borders are unclear, as, for example, hydrogen bonds are said to have partial covalent character.[9] Some models' overlap with other types of bonding is also apparent, particularly when we try to distinguish between certain types with different names when they are essentially the same.[10] So, besides careful evaluation of the information that we possess, more sensitive tools are required to gain a deeper understanding of these interactions, providing more clarity on their differences and similarities.

Table 1. Typical bond strengths of intramolecular (blue) and intermolecular (red) interactions.[11, 12]

Bonding	Energy (kJ/mol)
Ionic	400 - 4000
Covalent	150 - 1100
Metallic	75 - 1000
Ion-dipole	40 - 600
Hydrogen Bond	**10 – 40**
Halogen Bond	**1 - 40**
Dipole-dipole	5 - 25
Ion-induced dipole	3 - 15
Dipole-induced dipole	2 - 10
Dispersion (London)	0.05 - 40

However, most intermolecular interactions are weak, and this makes detecting and characterising them a challenge. This challenge is further exacerbated when measuring these interactions in solution, as solvents introduce additional competition and disorder as compared to the solid state. Accordingly, very weak non-covalent interactions detected by crystallographic techniques or predicted by computations may be impossible to characterise in dilute solutions. This thesis addresses the issue at hand by presenting a new nuclear magnetic resonance (NMR) methodology to characterise weak interactions in solution using hydrogen- and halogen-bonding as examples (Papers I & II). It also presents a thorough NMR-based investigation into the evidence of (or lack thereof) a new type of weak nucleophilic iodonium interaction (NII) in solution (Paper III).

1.1 Hydrogen Bonding

Hydrogen bonding (HB) has been comprehended, to some extent, for around a century.[13] Despite early advances around the turn of the 20th century, it was not until 1935 when Linus Pauling explicitly coined the term 'hydrogen bonding' for the first time.[14] Then, in 1939, he brought this interaction to the attention of many with his chapter on 'The nature of the chemical bond,' where

he defined it as a bond arising from electrostatics and gave more specific conditions for it to exist.[15] Since then, the debate as to what constitutes a HB has been ongoing, and various updates to this definition have been proposed.[16] HB became more generally defined, as more and more HB's were shown to violate previously existing conditions. In fact, the last of these updates was made as recently as 2011,[17] suggesting that we still do not know everything about HB and what constitutes it.

Contrary to what one may first think, HB's are formed between a HB donor, a species that contains a hydrogen (H) that is covalently bound to a more electronegative atom (X), and another electron-rich atom (Y; a HB acceptor), either within (being intramolecular) or between molecules (being intermolecular) (Figure 1),[18] attached to Z.
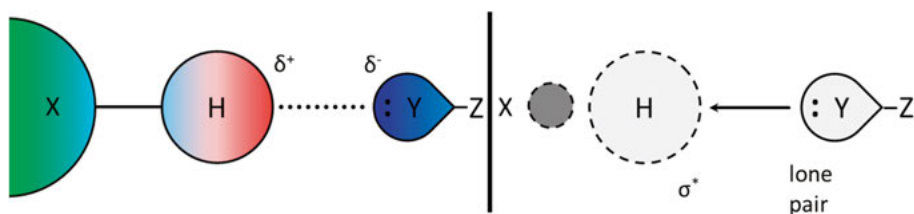

Figure 1. A hydrogen bond, showing both electrostatic (left)[19] and charge transfer (right)[16] models.

IUPAC, responsible for this latest 2011 definition, gave (six) criteria that can be used as evidence for HB formation.[17] HB is primarily an electrostatic, permanent dipole-dipole interaction between molecules or areas thereof, and they tend to be the strongest of all intermolecular interactions. They typically contain lesser charge transfer and dispersion components too. Due to a covalent bond between X, being electronegative, and H, the X−H bond is polarised and thus, HB bond strength increases upon the increase in electronegativity of X.

HB's are also specific in the sense that they can only occur between a hydrogen-containing HB donor and a relatively electron-rich HB acceptor (or electron donor), at an angle close to 180°. This means they are highly directional, and the closer to this linearity a HB can be, the stronger and consequently shorter it will be. HB's can be easily evidenced, primarily through vibrational techniques, by the extent of lengthening of a X−H bond and the creation of a new X−H···Y bond with its own vibration. Creation of a HB also drastically changes the electronic environment around the interacting proton. Through use of NMR spectroscopy, pronounced deshielding of this proton, a change in or appearance of through-bond couplings, and through-space effects, in particular NOEs, can easily be observed. And in general, to experimentally detect

a HB or any other weak interaction, the Gibbs energy of it should exceed the thermal energy of the system.

In the first classification of a HB, X only involved electronegative nuclei, though since then, multiple HB's have been detected where X is less electronegative, for instance, with carbon.[20, 21] The definition of the nucleophile, Y, has also changed over the years to incorporate other systems (for example, π-interactions), whilst Z has remained diverse, with electron donating groups affording better HB propensities on Y, and Z sometimes being absent altogether in instances where Y is a single-atom anion.

Typically, HB's are categorised into 3 main types: weak (< 17 kJ/mol), strong ($17 < 63$ kJ/mol) and very strong ($63 < 167$ kJ/mol).[22] Their bond lengths should not change depending on their environment, they should shorten as the ΔpK_a of their components gets smaller and their formation is favoured in non-polar solvents, though this does not necessarily mean that HB's are more stable in them.[23] Characterising weaker HB's in solution may prove challenging; their limits and strategies to enhance their resolution are therefore discussed herein.

1.2 Halogen Bonding

Halogen bonding (XB) was first observed as early as 1814,[24, 25] and was rationalised further 50 years later.[26] Over the next century, various advances were made in the field, including Mulliken's Nobel Prize-awarded work on molecular orbitals and the observation of charge transfer in halogen-bonded complexes through UV-Vis spectroscopy.[27, 28, 29] However, it was first Odd Hassel who put XB in the spotlight in 1969[30] when he disclosed the crystal structures of Br_2 halogen bonding with the oxygens of 1,4-dioxane and with π-electrons of benzene.[31, 32, 33, 34] The field remained largely stagnant throughout the next 30 years, before going through its renaissance around the turn of the new millennium. As recently as 2013, IUPAC provided its first official definition as "*a net attractive interaction between an electrophilic region associated with a halogen atom in a molecular entity and a nucleophilic region in another, or the same, molecular entity.*"[35, 36] Moreover, the distance between the interacting partners undoubtedly must be less than the sum of each component's van der Waal's radii.[37]

XB's are analogous to hydrogen bonds in their naming, where the electron donor is the halogen bond acceptor, and the halogen bond donor is an electron-deficient halogen atom that acts as electron acceptor.[38] This definition is contrary to that generally used in organic chemistry, as the electron donor is termed the "acceptor." Group 17 elements thereto are typically thought of as

only being electronegative leaving groups.[39] However, the same halogen is capable of acting also as electron acceptor, not just as an electron donor.

Much debate has recently taken place over the true nature of XB, mostly concerning if either the contribution of electrostatics or the charge transfer component dominates. The electron density distribution on a covalently bound halogen[40] indicates a region of positive electrostatic potential opposite a covalent R−X σ-bond, and is defined as a 'σ-hole'[41] (Figure 2). The charge transfer interpretation,[28] complimentarily, indicates that partial electron transfer occurs from a Lewis base's HOMO to a halogen's σ* antibonding LUMO, creating in some effect a 'charge-transfer complex.'[42, 43] Other notable contributions include polarisation and dispersion effects,[44] and under ideal circumstances, the bond has a 180° angle, with increasing deviations resulting in its weakening.

Classical XB's are observed between R−X···Y, where 'R' is any species covalently bound (usually through a carbon atom) to 'X,' the halogen atom, showing a halogen bond to a Lewis base, 'Y,' as in Figure 2. The strength of a XB can be tuned by withdrawing electron density from the halogen, for example, through perfluorination of R. This allows a more electropositive σ-hole, and thus a stronger XB.
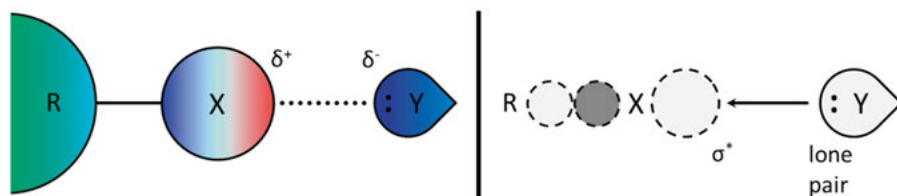

Figure 2. A halogen bond showing both electrostatic (left)[41, 45] and charge transfer (right)[28, 29] models.

The strength can also be tuned by increasing the XB donor ability, in the order I > Br > Cl >> F. This is explained by the decreasing electronegativity and increasing polarisability of the halogen atom when descending Group 17. Alternatively, XB can be strengthened by employing stronger Lewis bases (Y), and much alike HB, these can come from neutral species possessing non-bonding or lone pairs of electrons, π-electron systems,[46] or from anions.[47]

The halogen bond can further be strengthened by making the halogen a stronger Lewis acid by its oxidation to a halogen(I), forming a halonium ion (X^+). The earliest example of this was found in trihalide systems,[48] where the central halogen atom may act as an X^+ ion that interacts with two halide anions

(electron donors, 'D') in a linear $[D-X-D]^+$ arrangement.[4] To date, Br^+ and I^+ have shown consistent results in forming $[D-X-D]^+$ systems, whereas halogen bond complexes of F^+ and Cl^+ have been observed only at low temperatures (-80 °C and -35 °C, respectively), due to their high reactivity.[49] This type of XB, especially if non-halide, bidentate, electron-donating systems are involved, can exhibit interaction strengths of up to 180 kJ/mol.[50] The halogen bonds of halonium ions are unusually strong due to the 3-center 4-electron (3c4e) character of the bond, and to the halonium ion being a charged and thereby strong halogen bond donor. However, due to the abundance of electron density confined to p_x and p_y orbitals on the X^+ ion, this negative belt can, in theory, be considered as having electron donor qualities (Figure 3).
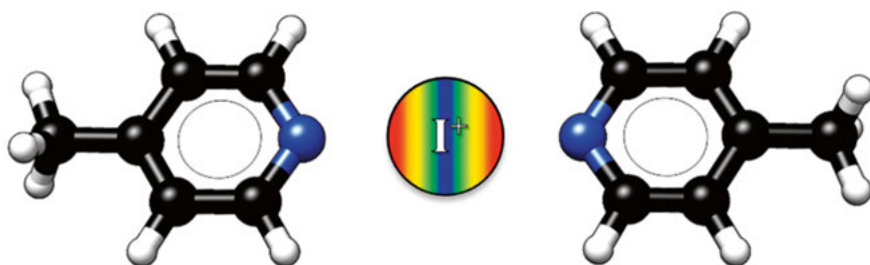

Figure 3. 3c4e halogen bond of I^+ showing its electron density distribution, with blue being an electron-rich belt and red signifying electron-poor regions of I^+ confined to a p_z orbital.

Many similarities exist between XB and analogous HB, but a few key differences can be noted between the two. XB's are more directional than their HB counterparts, due to repulsion of halogen lone pairs and a nearby Lewis base.[51] XB's are also more tuneable,[52] prefer softer Lewis bases, and are often better solubilised by apolar solvents due to their more hydrophobic nature and constituents.[53] Underpinning this is the fact that HB is largely dominated by electrostatics, whereas XB has a larger associated charge-transfer component,[12] most likely allowing it to be more resistant to polar (protic) solvents.[54, 55]

Most chemical reactions and biological processes take place in solution, and therefore, the understanding of halogen and hydrogen bonds and further weak interactions in solution is of great interest.[56, 57]

1.3 Characterising Weak Interactions in Solution

A variety of techniques have historically been used to characterise weak, non-covalent interactions in solution. Their capabilities for characterising weakly bound complexes under real-life like conditions, however, differ widely. As one of the main aims of this thesis work is to develop a new technique superior to those existing, and the second aim is to re-investigate a recently developed very weak interaction in solution, a short overview of the current spectroscopic techniques is given below.

Optical spectroscopies are inexpensive, comparably simple to use and are superior for the investigation of dilute solutions. However, they do not provide in-depth atomic level information and accordingly, they are nowadays rarely used for thorough studies of HB/XB in solution, but more as a complementary tool to NMR.[58, 59] Infrared (IR) and Raman spectroscopies, which are vibrational techniques, have been utilised for, as an example, characterising the XB of perfluoroalkanes,[60, 61] and to support results obtained through NMR studies.[62, 63, 64] Whereas they allow the detection of the formation of specific bonds at low concentrations, they are less commonly used nowadays, as they are limited by signal overlaps (several hydrogen bonds formed simultaneously, for instance) and as they are limited in providing atomic-level information, especially for larger complexes.

Electron spin resonance (ESR) spectroscopy is another technique that is occasionally used for characterising weak, non-covalent interactions. Nevertheless, it has great limitations as one can only study HB or XB interactions with stable organic radicals used as the Lewis base, such as the nitroxide nucleophile of TEMPO.[65, 66] Alternatively, ESR can be used applying 'spin probes' which act as indirect paramagnetic labels; these induce changes in hyperfine shift that can be followed over the course of a titration experiment.[67, 68] Whereas helpful for specific cases, ESR is limited by lack of general applicability for the investigation of non-covalent forces.

Nuclear magnetic resonance (NMR) spectroscopy is undoubtedly the most powerful technique for solution studies of non-covalent interactions. Its main advantage lies in its diversity, with multiple nuclei that are able to be probed in a variety of direct and indirect detection methods, through bonds or through space. These can be used alone or in combination with one another, so to derive structural, thermodynamic and/or kinetic information of any potential complexes held together by weak interactions.[69] However, it is limited by its sensitivity to lower concentrations as compared to aforementioned spectroscopies, for instance.

Isothermal calorimetry (ITC) measures the gain or loss of heat upon titration of one species into another in comparison to a reference, allowing the elucidation of the thermodynamics and stoichiometry of a binding process. As a high-sensitivity technique, it too is capable of measuring small changes upon binding in solution. However, it too suffers from a lack of atomic-level information and, as a result, cannot be used to distinguish exactly the type of interaction and the location at which it possibly takes place.

Whereas a single method may provide ample information on a non-covalent force, a multifaceted approach combining information from several independent methods is preferred. Hence, optical, vibrational, ESR and NMR techniques are best used in conjunction with one another. In addition to these, supporting: calorimetric (*e.g.* ITC), mass spectrometric (MS), X-ray diffraction (XRD) and/or computational (usually at the density functional theory (DFT) level) methods are recommended to complement any spectroscopic data.

1.4 Methods

Throughout this thesis, NMR titration and diffusion experiments have been applied and are therefore shortly introduced herein.

Titration experiments. In solution, weakly bound complexes exist in equilibrium. They typically exist in a fast-exchange regime on the NMR timescale, and the observed signal is a time-average of the signal of their complexed and their dissociated components; the strength of the interaction can be characterised by tracking this time-averaged signal. Ideally, separate samples are prepared by varying the concentration of one interaction partner, keeping the overall volume and ionic strength constant.[55] As one typically has access to a limited amount of at least one of the interaction partners, the preparation of separate samples often is not an option. Therefore, can be more convenient to carry out successive additions of a guest solution to the solution of the host, while tracking the relative concentrations of both. This, however, leads to dilution of the sample overall, changing its total ionic strength and the concentration of the host throughout the experiment, thus potentially influencing the results.[70] Using an excess of one binding partner and measuring its effect on the other maximises the fraction of complex in solution. In the case that the solvent is chosen as the interacting partner in excess, then the total concentration of complex will be maximised.[71, 72]

Throughout a titration, the changes of the chemical shift ($\Delta\delta$, ppm) of one or both interaction partners is followed. Variations of this rather simple methodology exist, namely in 'van't Hoff,'[73] and 'Chemical Double Mutant' approaches.[74] In the former, variable temperature (VT) NMR is employed at

each titration point, so to extract separate enthalpic and entropic terms. In the latter - where four highly similar species are measured with the presence of both, only one, only the other, and of neither interacting partner - the strength of binding is deduced by calculating the difference between the four experiments.

Titrations using a variety of nuclei other than ^{1}H, typically ^{19}F, ^{13}C, and ^{15}N can be advantageous for the characterisation of weak interaction forces. ^{1}H NMR is most popular due to a high abundance of ^{1}H nuclei on both Lewis bases and HB/XB donors. ^{19}F NMR has gained considerable use in the investigation of halogen bonding due to a high prevalence of perfluorinated XB donors which tend to be especially strong. In contrast, ^{13}C and ^{15}N nuclei remain less used due to their low sensitivity and natural abundance, although they may provide the most direct information; for instance, by tracking the chemical shift of the carbon holding a XB donor halogen atom,[75, 76] or the Lewis basic nitrogen that often takes part in an interaction.[77] The chemical shifts of these nuclei are therefore often observed by indirect detection experiments, such as HMBC, which provides vastly improved sensitivity. ^{1}H,^{15}N HMBC experiments have accordingly been used to characterise halogen bonding involving pyridine nitrogen atoms as halogen bond acceptors.[78] The halogen bond-induced chemical shift change, $\Delta\delta$ (ppm), of the ^{15}N nucleus typically is < 20 ppm for classical XB's[79] but may reach up to ~100 ppm in magnitude for the strongest XB's.[80] Needless to say, this is larger than the typically <1 ppm changes observed in titration experiments that use ^{1}H NMR for detection.

It should be noted that the choice of solvent has a pronounced influence on titrations, as solvent molecules vastly outnumber either interacting partner in solution. Polar solvents are required to dissolve most HB and XB systems,[81] often competing with these interactions in the process. Accordingly, when studying interactions that may suffer from solvent competition, typically aprotic solvents should be selected if at all possible.[82]

In order to determine binding strength in titration experiments, the stoichiometry of binding must be known and/or determined, with 1:1 binding solely being the case described throughout this thesis. Next, it must be known if the host-guest complexation equilibrium is in either slow or fast exchange regimes, with the latter being the case with weak binding (as in this thesis). Estimating the association constant beforehand can also be helpful, with $K_a > 2$ M^{-1} being considered a favourable interaction, and $K_a > 10$ M^{-1} being more reliable to measure.[83]

The stoichiometry of the adducts can be determined through Job's method,[84] though these have recently fallen out of favour,[85] although this method is also applicable to titration data.[86, 87]

Diffusion NMR uses a series of 'pulsed-field gradient spin echo' (PGSE) spectra and measures the rate of signals' decay.[88, 89] This provides a molecule's rate of translational motion in solution, described with the 'diffusion coefficient' (D_t). Generally, the smaller a molecule is, the less solvent-accessible molecular surface area it has, so the less it interacts with the solvent and the quicker it diffuses. This molecular motion is described by the Stokes-Einstein equation, Eq. 1:

$$D_t = \frac{kT}{6\pi\eta r_H} \tag{1}$$

where D_t is the diffusion coefficient of the molecule/adduct, k is the Boltzmann constant, T is the absolute temperature, η is the fluid viscosity and r_H is the hydrodynamic radius of the molecule/adduct. By default, this equation describes spherical objects, though adjustments can be made to correct for smaller, flatter and less-spherical species.[90] Diffusion-ordered spectroscopy (DOSY) experiments give pseudo-2D spectra with chemical shifts on the f2 (x) axis and diffusion coefficients on the f1 (y) axis. Thus, they allow the simultaneous detection of a number of species in a sample, provided they each have different diffusion coefficients;[91] overlapping signals may then be separated.

1.5   Limitations of Current Methods

Despite all advances made in characterising weak interactions in solution, limitations still exist. Interactions with strengths of <6 kJ/mol[83, 92] are difficult to detect using routine NMR spectroscopic techniques due to solvent competition, entropy, and the overall lower molar fraction of the bound species of weakly binding complexes in dilute solutions.[93]

Thus far, most studies focus on optimised and idealised molecular systems that possess high association constants to avoid the limitations of current techniques. Strategies that reduce entropic costs upon binding, such as employing intramolecular bonds[94, 95] and multidentate systems,[96, 97] are thus rather common. Investigations in polar, protic solvents are rare as these may, in most instances, compete with HB/XB of the interaction partners.[12, 98] Furthermore, high concentrations of binding partners are typically used to increase the molar fraction of the bound complex. If the bound fraction is below 20% (or above 80%), propagation of errors may lead to unreliable K_a determination.[83,

[99, 100] Furthermore, other complexes of weakly bound species can exist in the NMR sample, perhaps with the solvent,[12, 101] further complicating binding phenomena observed and casting ambiguity over results obtained.

Whereas studies of strongly binding systems at high concentrations in non-polar solvents are ultimately easier, they are often far from the real-life conditions of medicinal and synthetic chemistry. Therefore, a valuable contribution to the field would be the development of a novel technique that has its strengths where current methods have their limitations, allowing the study of weaker bonds at lower concentrations and in more polar solvents.

1.6   Aim of Thesis

This thesis aims to lay the basis for a new strategy that allows the detection of weak non-covalent interactions in solution by making use of paramagnetism-affected NMR observables (Chapter 2; Papers I and II). The scope of this technique is explored by the detection and characterisation of weak HB's through paramagnetic tagging of a Lewis base and detection of 'transferred paramagnetism-affected observables' on the interacting Lewis acid (Chapter 3; Paper I). The opposite approach is also explored by paramagnetic tagging of a XB donor and detection of transferred paramagnetism-affected observables on the diamagnetic interaction partner, a Lewis base (Chapter 4; Paper II). The last section aims to re-investigate a recently proposed 'Nucleophilic Iodonium Interaction' in solution (Chapter 5; Paper III), to evaluate whether it truly exists.

2. The Paramagnetic NMR Technique (Papers I & II)

2.1 Paramagnetism in NMR Spectroscopy

In this thesis, a new technique is developed that makes use of paramagnetism-affected NMR observables. Accordingly, a short introduction into paramagnetic NMR observables is given below.

When unpaired electrons are present as a component of a sample, profound paramagnetic effects can be observed on the NMR spectra.[102] This is due to the extraordinary magnetic moment that an electron possesses, around 660 times that of a proton's.[103] Paramagnetic effects are of through-space and of long-range character, and can be detected up to 40 Å from the unpaired electrons,[104] being at much larger distances than NOEs can ever reach (<5-6 Å).

The paramagnetic observables of current highest importance are the *(I)* increased T_2 relaxation rates, commonly termed 'paramagnetic relaxation enhancement' (PRE), *(II)* the changes in chemical shifts leading to 'pseudocontact shifts' (PCS), and *(III)* the alteration of the magnitude of *J* couplings, known as 'residual dipolar coupling' (RDC).[105]

PRE is governed by 'Solomon Relaxation' and 'Curie Spin Relaxation.'[106] Both independently and combined, they give r^{-6} distance dependent information on the position of nuclear spin in relation to an unpaired electron. PRE can typically be detected 5-20 Å from the paramagnetic source depending on the dominating mechanism of relaxation,[107] and is commonly quantified by the increase of width-at-half-height of NMR signals (Figure 4), as compared to a diamagnetic reference.

PCS is the distance and orientation dependent change in chemical shifts of nuclei in the vicinity of unpaired electrons upon a paramagnetic species, and these arise due to the magnetic field generated by an electron's anisotropic static magnetic moment. In the presence of a paramagnetic nucleus, the magnetic field experienced by various nuclei are not entirely averaged by molecular rotation. This leads to the observation of PCS's[108] that are described by Eq. 2:[109]

$$\Delta\delta^{PCS} = {}^{1}\!/_{12\pi r^3}\left[\Delta\chi_{ax}(3cos^2\theta - 1) + 1.5\Delta\chi_{rh}sin^2\theta cos2\phi\right] \qquad (2)$$

where PCS, measured in ppm, is dependent upon the distance (r^{-3}) and also the angle (θ, ϕ) at which a nucleus lies in respect to the principal axis frame of a paramagnetic metal's magnetic susceptibility anisotropy tensor ($\Delta\chi$). An anisotropic chi-tensor, $\Delta\chi$, can be subdivided into separate axial ($\Delta\chi_{ax}$) and rhombic ($\Delta\chi_{rh}$) components–the magnitude of these depending on the paramagnetic centre (Figure 5).[110] PCS has profound effects on the chemical shift and hence on the spectral window observed, with simple ^{1}H spectra of some lanthanide complexes spanning up to hundreds of ppm. Similar to other paramagnetism-affected NMR observables, PCS is the change of chemical shift upon introduction of a paramagnetic centre, and thus, it is measured in comparison to a diamagnetic reference.

RDC is the change of a dipolar coupling, most often detected on J coupling, due to orientation of a compound in a strong magnetic field.[111] This may be due to introduction of an unpaired electron into a molecular system, and affords information on the alignment tensor ($\Delta\chi$) and on the orientation of a vector connecting two spins (A and B) in a magnetic field. RDC's are most often detected in an f2-coupled HSQC spectrum and are measured as a difference of the scalar coupling ($^{1}D_{AB}$) measured for an anisotropic (aligned; $^{1}T_{AB}$) and an isotropic (unaligned; $^{1}J_{AB}$) sample. The RDC is described by Eq. 3.[112]

$$RDC_{AB}(Hz) =$$
$$-\frac{1}{4\pi}\frac{B_0^2}{15k_BT}\frac{\hbar\gamma_A\gamma_B}{2\pi r_{AB}^3} \times \left[\Delta\chi_{ax}(3cos^2\Theta - 1) + 1.5\Delta\chi_{rh}sin^2\theta cos2\Phi\right] \qquad (3)$$

where B_0 is the external field strength, k_B the Boltzmann constant, T the absolute temperature, $\hbar$ the reduced Planck's constant, γ the gyromagnetic ratio of nuclei A and B, and r_{AB} the internuclear distance between these A and B spins. Angles θ, Θ and Φ are described in Figure 4,[113, 114] and represent the orientations of the A $\rightarrow$ B vector relative to the external field. To be able to identify the orientation of a compound in relation to the external field, five or more independent vectors are required.[115] The measurements necessitate the use of a diamagnetic/non-orienting reference, as RDC is the change in scalar coupling as compared to a non-oriented sample. RDC's may be obtained through use of alignment media;[116] however, in such a case no PRE or PCS can be obtained.
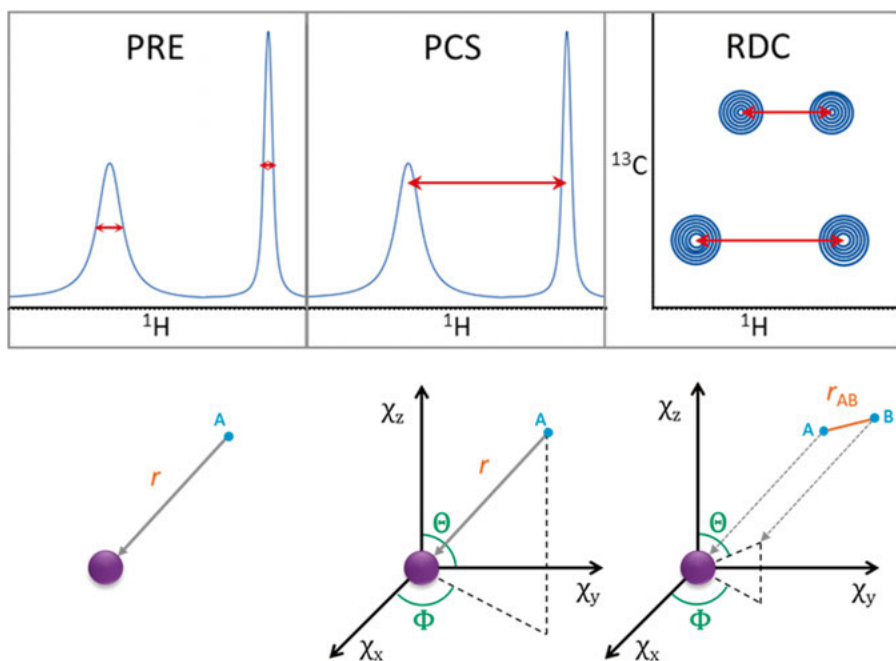
Figure 4. Paramagnetism-affected observables and their visualised components, with PRE (left) showing peak broadening and its distance dependence, PCS (centre) showing chemical shift change and its distance and orientation dependence, and RDC (right) showing a change in *J*-coupling in an f2-coupled ^{1}H,^{13}C HSQC spectrum and its orientation dependence.[105]

Due to an r^{-3} distance dependence of PCS's and RDC's, they can be detected over distances up to 40 Å,[104, 117] and their magnitude depends on the distance from unpaired electron(s), typically upon a paramagnetic centre, and quantifiable in terms of interatomic distance. To determine the $\Delta\chi$ tensor that describes the relative orientation as compared to the external field, a number of software are available, of which 'Paramagpy'[118] has been used herein.

A common approach to implementing a paramagnetic species into a system of interest is to use stable organic radicals, typically those involving nitroxides such as TEMPO.[119] Another approach takes advantage of transition metal ions' free, unpaired d-electrons. Depending on the nature of their complexing agents, these include physiologically inert Mn^{2+}, Fe^{2+}, Co^{2+}, Ni^{2+} and Cu^{2+} metal ions.[120] A disadvantage of using either approach is that it is difficult to incorporate chemically similar diamagnetic reference molecules/ions, and that (bar Co^{2+}) they typically possess an isotropic arrangement of unpaired electron(s) giving only PRE's. If they do happen to possess anisotropy of electrons, they are dominated by strong PRE whereas PCS's are small.[102] When

a paramagnetic species has an isotropic or spherical arrangement of electrons, the x, y and z components of $\Delta\chi$ are equal to zero and no PCS or RDC effects are observed, [107] only PRE.

Lanthanides are 'rare earth elements' that mainly exist as Ln(III) (or Ln(II)) salts in nature. They have up to 7 unpaired electrons in their valence 4f orbitals, which in turn are diffuse. As these electrons are shielded by 5s and 5p subshells, they are unreactive and do not tend to coordinate to ligands. When introduced to a magnetic field in an NMR spectrometer, these orbitals partially align with the magnetic field, B_0, and display the aforementioned paramagnetic effects. Figure 5 shows the isosurfaces constructed from positive (blue) and negative (red) PCS's, representing the $\Delta\chi$ tensor overall.[121] Relative PRE, ground state (J), the χ-tensor and its axial and rhombic components, and electron relaxation times (τ_e; at 18.8 T magnet strength) are also shown; promethium is omitted due to its radioactivity.

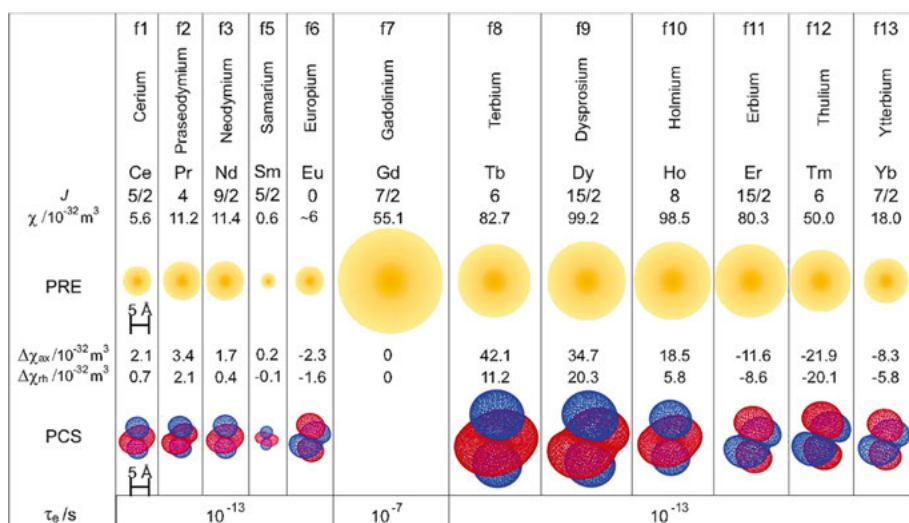|	f1	f2	f3	f5	f6	f7	f8	f9	f10	f11	f12	f13
	Cerium	Praseodymium	Neodymium	Samarium	Europium	Gadolinium	Terbium	Dysprosium	Holmium	Erbium	Thulium	Ytterbium
	Ce	Pr	Nd	Sm	Eu	Gd	Tb	Dy	Ho	Er	Tm	Yb
J	5/2	4	9/2	5/2	0	7/2	6	15/2	8	15/2	6	7/2
$\chi\,/10^{-32}\,m^3$	5.6	11.2	11.4	0.6	~6	55.1	82.7	99.2	98.5	80.3	50.0	18.0
PRE												
$\Delta\chi_{ax}/10^{-32}\,m^3$	2.1	3.4	1.7	0.2	-2.3	0	42.1	34.7	18.5	-11.6	-21.9	-8.3
$\Delta\chi_{rh}/10^{-32}\,m^3$	0.7	2.1	0.4	-0.1	-1.6	0	11.2	20.3	5.8	-8.6	-20.1	-5.8
PCS												
τ_e/s			10^{-13}			10^{-7}			10^{-13}			

Figure 5. A summary of trivalent lanthanide ions' properties. Reprinted with permission from *Acc. Chem. Res.* **2007**, *40*, 206-212. Copyright 2007 American Chemical Society.

The paramagnetic effect varies depending on the Ln^{3+} ion used (Figure 5). Due to the fact that most trivalent lanthanide ions have comparable ionic radii and highly similar reactivity, the paramagnetic effect can be tuned by exchanging ions, without any larger changes in geometry.[122]

Diamagnetic trivalent lanthanide ions exist with no f-electrons (lanthanum(III)) and with full f-electron orbitals (lutetium(III)). These are ideal for

use as diamagnetic reference ions in studies where paramagnetic effects are measured. Gadolinium(III) possesses an isotropic arrangement of 7 unpaired electrons, and has exceptional relaxation-enhancing properties yielding a large PRE but no RDC's or PCS's.[123] All trivalent lanthanides have the potential to be incorporated into systems suitable for NMR studies, primarily through ionic and coordinative bonding to complexing agents.

The fact that PCS's and RDC's can be observed even at large distances from a paramagnetic centre, and that their magnitude is distance and orientation, or orientation dependent, respectively, provides useful tools for the assessment of weak interaction forces. As their magnitude is larger as compared to typical binding induced chemical shift changes, they can be accurately detected, with the measurement error being comparatively low.

2.2   Lanthanide (III) Complexing Agents

The strongest metal complexing agents are multidentate and produce stable complexes, with trivalent lanthanide ions forming 8/9-coordinate complexes.[124] Early examples of Ln^{3+} ligands include ethylenediaminetetraacetic acid **1** (EDTA)[125] and diethylenetriaminepentaacetic acid **2** (DTPA).[126] Ln-complexes with texaphyrins have also seen use,[127] whereas the lanthanides can be complexed by a metalloprotein of interest, often being a viable substitute for Ca^{2+} ions, for example.[128] 1,4,7,10-tetraazacyclododecane **3** (cyclen) and 1,4,7-Triazacyclononane **4** (TACN) complexes are most used nowadays due to their favourable cavity sizes and their ability to be substituted with various pendant 'arms' (R) which allow full coordination of Ln^{3+} ions, typically in a tricapped trigonal prismatic geometry for commonly tri-substituted TACN metal complexes described hereafter.[129]
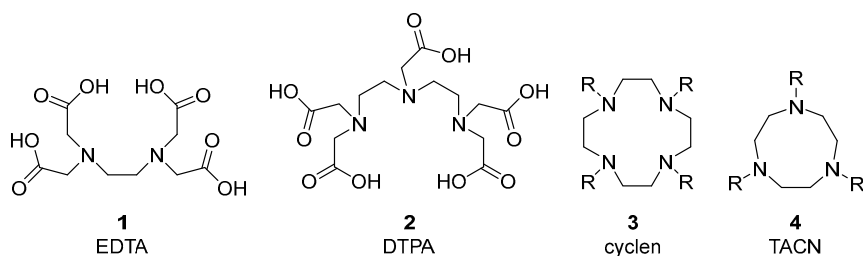

Figure 6. Common lanthanide complexing agents.

These complexes can, for instance, be added to a solution of interest to map protein surfaces and dynamics,[130, 131] or as contrast agents in medical magnetic resonance imaging (MRI), typically Gd-DOTA (**5**) cyclen derivatives.[132, 133] They can also be covalently bound to a protein of interest (**6**), allowing its investigation through use of paramagnetism-affected NMR observables. PRE, PCS's and RDC's may then be used to map changes in the protein's conformation, or to characterise the binding of other proteins[134] or small molecule inhibitors to it.[135] Small molecules have also been tagged,[136] and the protein binding site of a small molecule ligand was mapped using a paramagnetic tag (**7**),[137] providing the first example of anisotropic paramagnetic properties transferred through a specific binding event.
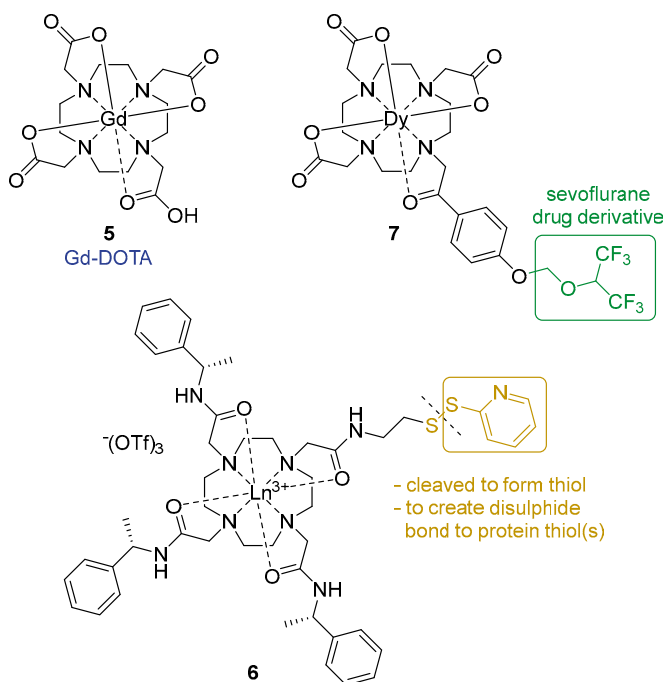
Figure 7. Examples of lanthanide(III) complexes containing a cyclen core structure that are used for different purposes.

The applicability of paramagnetic NMR for the understanding of weak non-covalent forces between small molecules has, however, not yet been explored. This approach is expected to be advantageous as the magnitude of PCS is larger than the chemical shift changes that are induced by binding of small molecules, and RDC's may provide long distance orientation information that would not be available from other NMR parameters, such as NOE's. The goal in this work is to explore whether paramagnetic NMR can be used to examine

single, weak non-covalent interactions under conditions that are not possible with the current standard NMR techniques.

2.3 Strategy

To study a weak non-covalent interaction between two small molecules in solution *via* paramagnetic NMR, one of the components has to be paramagnetically labelled. Binding of the second diamagnetic component to the paramagnetic interaction partner results in its orientation, and thus, allows one to detect paramagnetism-affected NMR observables on the bound diamagnetic substance. Comparison of this binding event to that with an almost identical diamagnetic complex allows deduction of these paramagnetism-affected NMR observables. Employing small molecules that instead do not bind should result in no paramagnetism-affected NMR observables (Figure 8). This strategy is explored herein by studying hydrogen and halogen bonds as model systems.
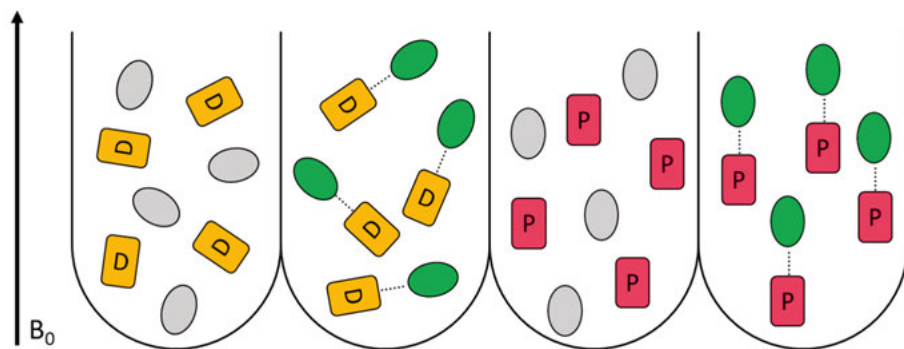
Figure 8. Non-binding molecules (grey) should not bind to either diamagnetic (D; amber) or paramagnetic (P; magenta) complexes. Molecules that bind (green), bind in an isotropic manner to diamagnetic complexes, and in an anisotropic manner to paramagnetic complexes, with respect to B_0. Paramagnetic complexes themselves show anisotropy even in the absence of any bound molecule.

Two approaches were taken to create functionalised lanthanide(III) complexes to probe HB and XB in solution. The first approach was to design a Lewis-basic complex (Figure 9) for the detection of paramagnetic observables on a diamagnetic HB or XB donor. This was explored through incorporation of a Lewis basic pyridine moiety covalently attached to the lanthanide(III) tag.
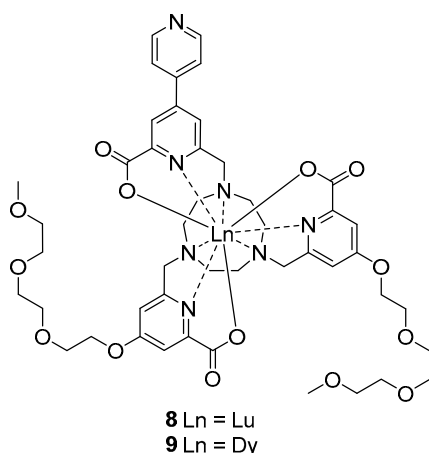
8 Ln = Lu
9 Ln = Dy

Figure 9. Target Lewis base-functionalised lanthanide(III) tag.

First a Lewis base was covalently bound ('tagged') to a lanthanide complex. As a Lewis base, pyridine was selected as it has previously been used to study HB/XB, is uncharged, sterically not hindered, and the electron donation through its lone pair is highly directional. The 'core' of the chelating molecule was chosen to be TACN as it provides a large enough cavity and three amine electron lone pairs for a Ln^{3+} ion to coordinate to. Each amine was substituted with a picolinate-based 'arm' to coordinate to the Ln^{3+} ion through a pyridine nitrogen electron lone pair and a carboxylate functional group. The resulting complex is neutral which provides solubility in less polar solvents and avoids interference of binding from counterions. Its lanthanide ion is nine-coordinated, which avoids the direct interaction of Lewis bases with the lanthanide ion. The Lewis basic pyridine was connected to one arm, with the pyridine nitrogen atom at a distance of 9.72 Å from the Ln^{3+} ion. The distance of the Lewis base from the paramagnetic centre is important to provide a large enough PCS to be detected on the interaction partner along with a minimal PRE that would decrease sensitivity due to line broadening. Dy^{3+} was chosen as the paramagnetic ion (**9**) as should induce large PCS's (Figure 5), whereas Lu^{3+} was chosen as the diamagnetic reference ion (**8**) due to its higher similarity to later-stage Ln^{3+} ions than La^{3+}. On the remaining two arms were polyethylene glycol (PEG) chains so to increase Ln-complex solubility in polar (non-protic) organic solvents, such as acetonitrile.

The second, opposite approach, was to design a Lewis acid-functionalised lanthanide(III) tag for the detection of paramagnetic observables on a diamagnetic Lewis base. This was explored on a system encompassing an iodoacetylene-type XB donor. This geometry, with 10.01 Å in between the lanthanide

and the iodine XB donor atom (Figure 10), is expected to allow measurable PCS's, based on previous studies.[136]
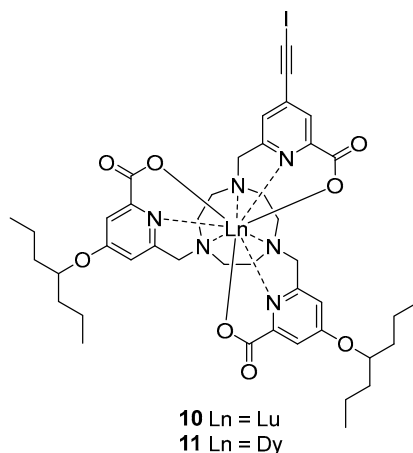

10 Ln = Lu
11 Ln = Dy

Figure 10. Target halogen bond donor-functionalised lanthanide(III) tag.

A TACN core with three picolinate-based pendant arms was designed, with one of these arms containing the XB donor atom. Iodine was chosen due to its superior ability to form XB's than other halogens, and was covalently bound through an acetylene group to an aromatic system, as this has been previously applied in studies of halogen bonding in solutions.[75, 76] The remaining two arms were substituted with heptan-4-yl chains to provide increased solubility in organic solvents. Lu^{3+} (**10**) and Dy^{3+} (**11**) were chosen as the diamagnetic and paramagnetic trivalent lanthanide(III) ions, respectively.

2.3   Synthesis of Lewis base-functionalised TACN Complexes

These complexes were constructed by first assembling the PEG-based (Scheme 1) and Lewis basic (Scheme 2) pendant arms, and then substituting the TACN molecule with these in a step-wise fashion, before carboxylic ester deprotection and lanthanide complexation (Scheme 3).
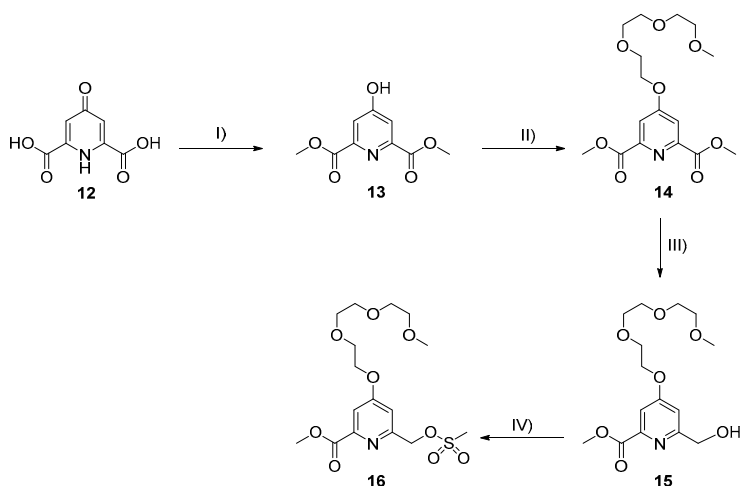
Scheme 1. Synthesis of PEG-based pendant arms to increase organic solubility. *I) H₂SO₄, MeOH, 80 °C, 24 h, 95%;[138] II) 1-(2-Bromoethoxy)-2-(2-methoxyethoxy)ethane, K₂CO₃, MeCN/DMF 2:1, 90 °C, 19 h, 71%; III) NaBH₄, MeOH/CH₂Cl₂ (3:1), 0-20 °C, 16 h, 60%; IV) mesyl chloride, NEt₃, CH₂Cl₂, 0-20 °C, 90 min, 98%.*

To produce organic-solvent solubility-enhancing arms (Scheme 1), chelidamic acid monohydrate was first esterified *(I)*, followed by a Williamson ether synthesis *(II)* to introduce a PEGlyated chain (**14**). Next, selective reduction *(III)* of one ester was achieved with careful control of reducing agent, NaBH₄, to give **15**. Mesylation *(IV)* of the resulting alcohol yielded **16**, with the mesylate group being a good leaving group for a following alkylation step.
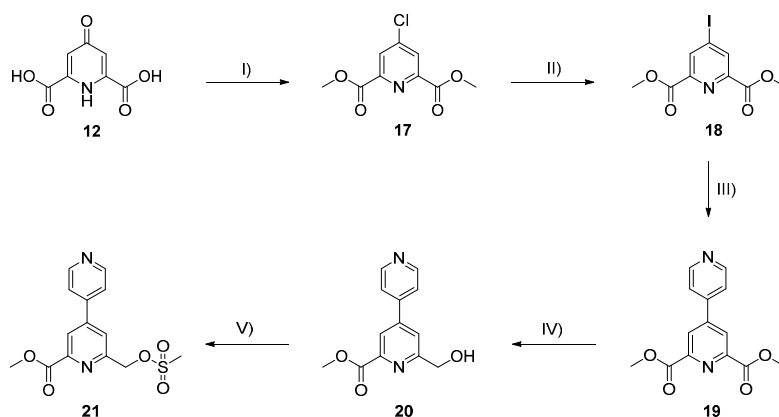
Scheme 2. Synthesis of Lewis basic pyridine pendant arm. *I) two steps: (1) SOCl₂, dimethylformamide (DMF), 80 °C, 24 h; (2) MeOH, 20 °C, 1 h, 75%;[139] II) NaI, acetyl chloride, 20 °C, 30 min, 81%;[140] III) PdCl₂(PPh₃)₂, 4-pyridinylboronic acid, K₃PO₄, DMF, 75 °C, 48 h, 58%; IV) NaBH₄, MeOH/CH₂Cl₂ (3:1), 0-20 °C, 16 h, 62%; V) mesyl chloride, NEt₃, CH₂Cl₂, 0-20 °C, 90 min, 97%.*

To generate the Lewis basic interaction site (Scheme 2), chelidamic acid monohydrate was chlorinated *(I)* with acyl chloride and esterified with MeOH to give **17**. This chloride was substituted for an iodide *via* a Finkelstein exchange reaction *(II)* in MeCN with sonication, providing a superior leaving group in the following reaction. A Suzuki cross-coupling reaction *(III)* was then carried out with **18** and 4-pyridinylboronic acid hydrate to yield **19**. Following this, a selective reduction *(IV)* of one ester group and mesylation *(V)* of the resulting alcohol gave **21**.
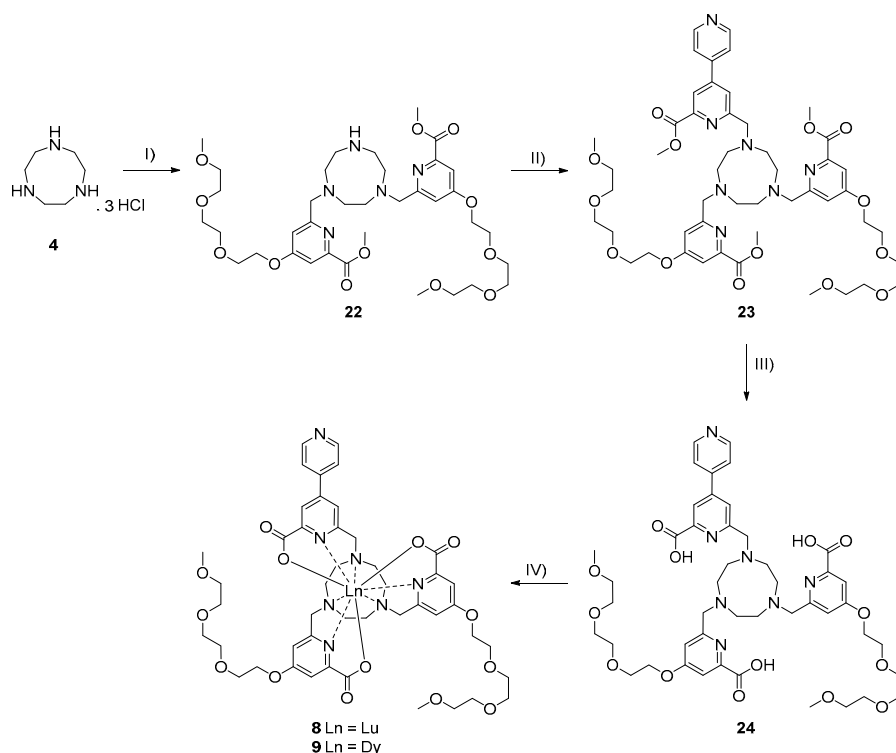
Scheme 3. Alkylation, acid deprotection and complexation of Lewis base-functionalised lanthanide(III) tag. *I) Compound **16**, NEt₃, CH₃CN, 50 °C, 72 h, 39%; II) Compound **21**, K₂CO₃, 20 °C, 48 h, 40%; III) NaOH (2M), THF/H₂O (3:2), 50 °C, 24 h, 21%; IV) LnCl₃, Na₂CO₃, H₂O, 20 °C, 16 h, 17-26%.*

To connect the 'arms' to the TACN core (Scheme 3), the HCl salt of TACN (**4**) was stirred in the presence of a base, DIPEA, to deprotonate the secondary

32

amines. Dropwise addition of two equivalents of the mesylated, PEGylated arms (**16**) gave **22** through an aliphatic *N*-alkylation reaction *(I)*. After purification, **22** was treated with K_2CO_3 as a base, and a similar alkylation reaction *(II)* was carried out to attach the Lewis basic pyridine-containing arm. Carboxylate esters of **23** were next hydrolysed *(III)* by use of a strong base, 2M NaOH. Lanthanide complexation *(IV)* of **24** with Na_2CO_3 as a base and the desired lanthanide chloride salts, $LuCl_3$ and $DyCl_3 \cdot 6 H_2O$, respectively, was performed. Purification by means of HPLC gave the final Lu (**8**) and Dy (**9**) complexes as white solids.

The ^{1}H NMR spectrum of diamagnetic lutetium complex **8** showed signals at $\delta = 0\text{-}10$ ppm, whereas the paramagnetic dysprosium complex **9** displayed a much larger chemical shift window of > 200 ppm (Figure 11). The lutetium complex (**8**) was fully characterised with NMR and HRESIMS, whereas the paramagnetic dysprosium complex (**9**) was characterised by means of ^{1}H NMR and HRESIMS.
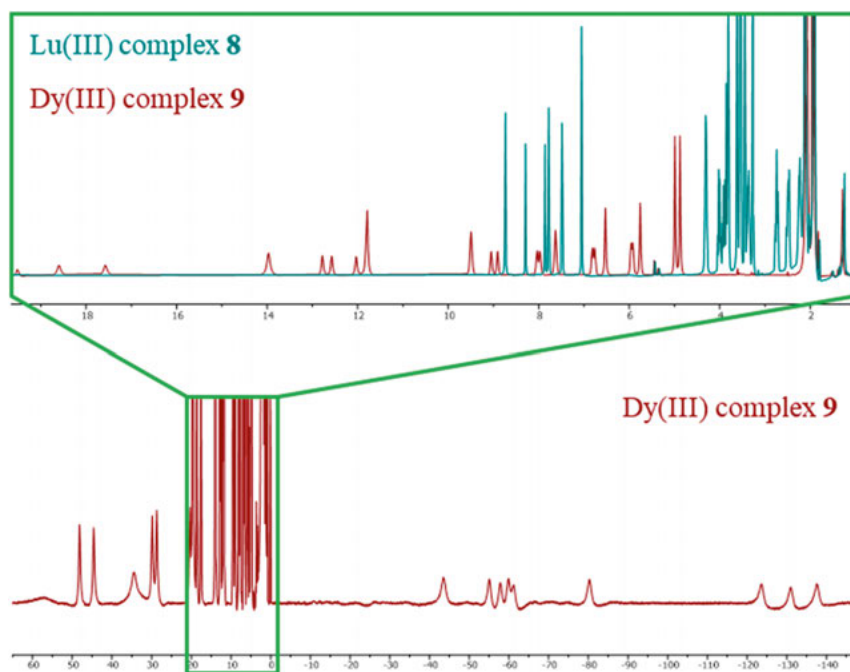

Figure 11. Lu complex **8** (top; teal) *versus* Dy complex **9** (top and bottom; maroon) ^{1}H spectra, showing the extent of PRE (line-broadening) and of PCS's ($\Delta\delta$ (ppm)).

In Figure 11, one can see an enormous increase in the chemical shift range due to PCS, and the large extent of line broadening due to PRE, upon the Dy(III)

complex **9** in comparison to the Lu(III) complex **8**. The extent of these para-magnetism-affected NMR observables is largest for nuclei closest to the Ln^{3+} ion.

2.4 Synthesis of Lewis Acid-functionalised TACN Complexes

The synthesis of this Lewis acidic or 'XB donor' system generally followed the same process as that of Compounds **8** and **9**, which possess a Lewis basic interaction site instead. First, arms that should allow enhanced solubility in organic solvents were constructed (Scheme 4), followed by the synthesis of an iodoacetylene-precursor arm (Scheme 5). Complexes were assembled by alkylation of TACN with these arms, deprotection of protecting groups, complexation with a lanthanoid salt, and addition of an iodide (Scheme 6).
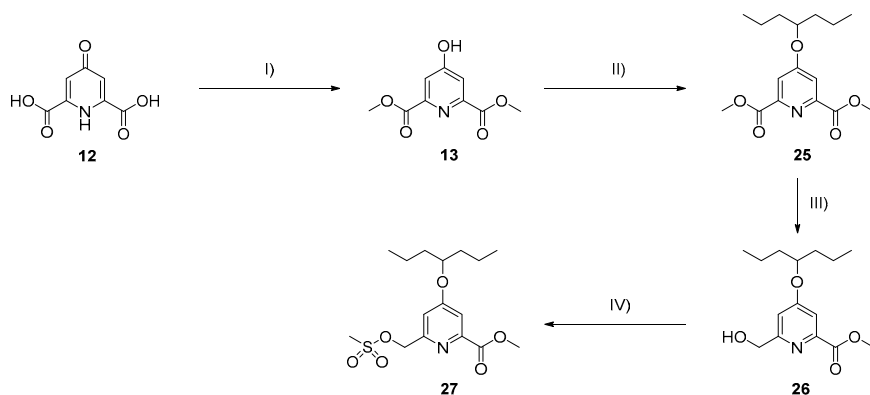

Scheme 4. Synthesis of organic solvent solubility-enhancing pendant arms. *I) H₂SO₄, MeOH, 80 °C, 24 h, 95%;[138] II) 4-bromoheptane, K₂CO₃, DMF, 70 °C, 20 h, 45%; III) NaBH₄, MeOH/CH₂Cl₂ (3:1), 0-20 °C, 16 h, 65%; IV) mesyl chloride, NEt₃, CH₂Cl₂, 0-20 °C, 90 min, 99%.*

To obtain organic-solvent solubility-enhancing arms (Scheme 4), chelidamic acid monohydrate was esterified *(I)* by use of a strong acid, H_2SO_4,[138] before substitution *(II)* with 4-bromoheptane to yield an ether, **25**. Careful mono-reduction *(III)* of a carboxylate ester with $NaBH_4$ gave **26**, which was then mesylated *(IV)* to give **27**.
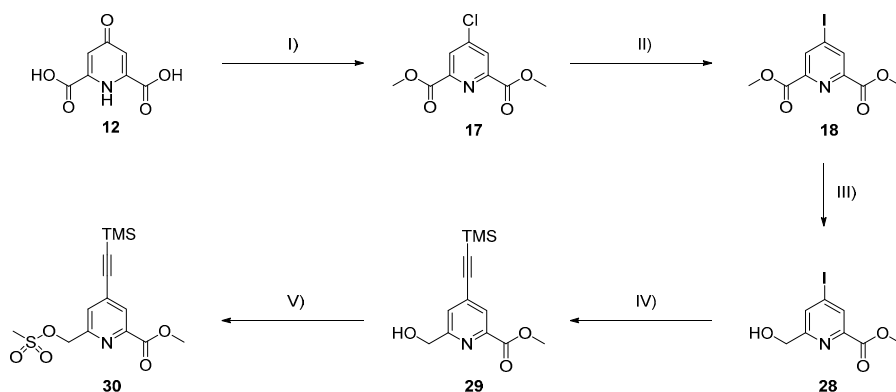
Scheme 5. Synthesis of protected acetylene pendant arm. *I) two steps: (1) SOCl₂, di-methylformamide (DMF), 80 °C, 24 h; (2) MeOH, 20 °C, 1 h, 75%;[139] II) NaI, acetyl chloride, 20 °C, 30 min, 81%;[140] III) NaBH₄, MeOH/CH₂Cl₂ (3:1), 0-20 °C, 16 h, 65%;[140] IV) CuI, NEt₃, PdCl₂(PPh₃)₂, TMS-acetylene, THF, Ar, 25 °C, 1h, 81%; V) mesyl chloride, NEt₃, 0 °C, 30 min, 99%.*

Subsequently, XB donor-containing moieties were primed (Scheme 5). Chelidamic acid monohydrate was once again used as the starting material, where upon esterification and chlorination *(I)*,[139] and then Finkelstein exchange *(II)*,[140] gave **18**. This was then mono-reduced *(III)* with careful addition of NaBH₄.[140] A Sonogashira cross-coupling reaction *(IV)* was performed with TMS-acetylene to yield **29**, which was then mesylated *(V)* to give **30**.
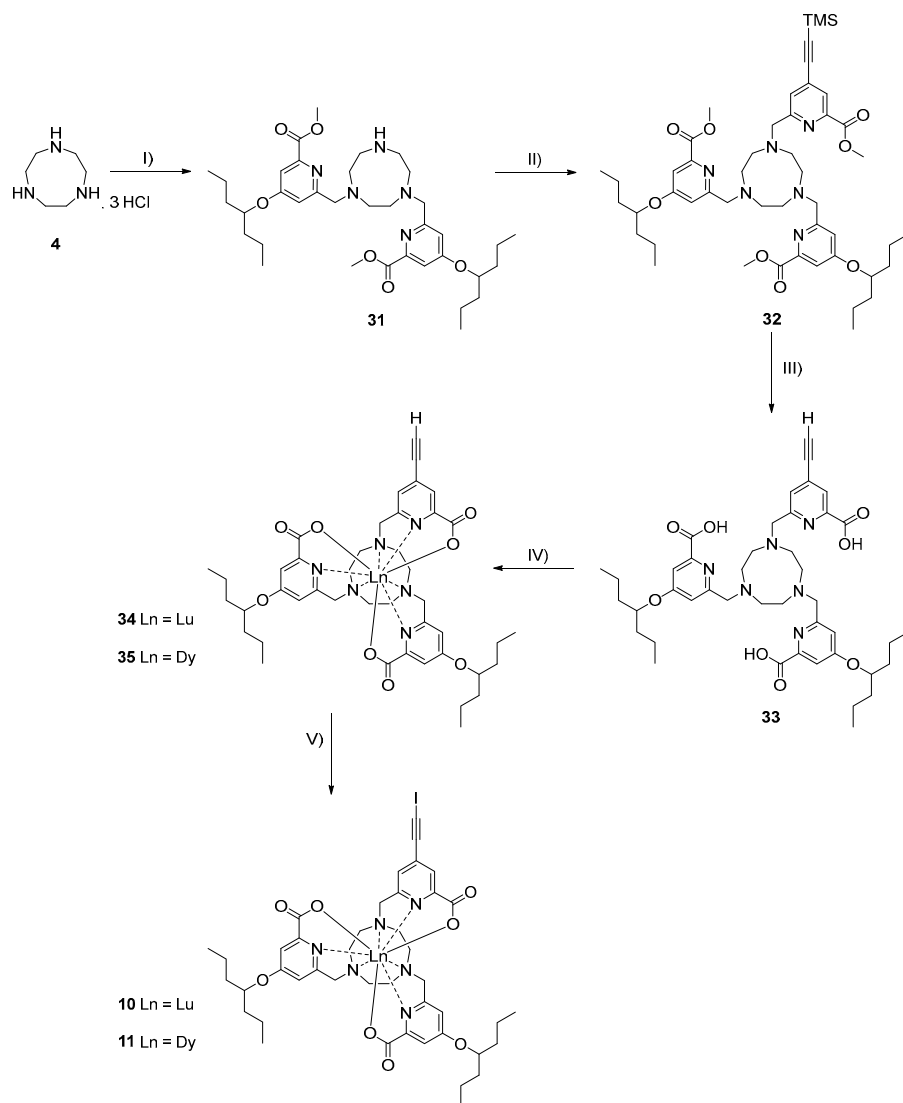
Scheme 6. Alkylation (×2), TMS-group deprotection, complexation and iodination of halogen bond donor tag. *I) Compound 27, NEt₃, CH₃CN, 20 °C, 72 h, 30%; II) Compound 30, NEt₃, 20 °C, 24 h, 37%; III) NaOH (2M), H₂O, THF, 50 °C, 24 h, 64%; IV) LnCl₃, Na₂CO₃, H₂O, 20 °C, 16 h, quantitative; V) AgNO₂, N-iodosuccinimide, acetone, 20 °C, 1 h, 55-58%.*

Alike before, these arms were attached to TACN under basic conditions (Scheme 6). An alkylation *(I)* with 2 equivalents of solubility-enhancing arms (**27**) was performed with NEt₃, before further alkylation *(II)* with the TMS-protected acetylene arm (**30**) in NEt₃, yielding **32**. Simultaneous carboxylate

and TMS deprotection *(III)* was achieved with use of NaOH (2M). Complexation *(IV)* of lanthanide salts, $LuCl_3$ and $DyCl_3.6 H_2O$, gave **34** and **35**, respectively, in presence of Na_2CO_3. A final iodination *(V)* of the acetylene group with *N*-iodosuccinimide was accomplished with $AgNO_3$ as the catalyst under dark, inert, dry conditions to yield **10** and **11** as white solids after HPLC purification. High resolution electron spray ionisation mass spectrometry (HRESIMS) and ^{1}H NMR confirmed the existence of both complexes, with the lutetium complex (**10**) additionally characterised by means of further NMR spectra.

2.5 Concluding Remarks

Taking inspiration from recent literature,[141] novel lanthanide-chelating complexes bearing Lewis basic or Lewis acidic (XB donor) functionalities were synthesised. Their purity was confirmed *via* HPLC, while their identity was confirmed by NMR measurements, with the lutetium complexes being fully characterised and the dysprosium complexes being verified by the effect of their paramagnetic properties on ^{1}H NMR spectra. These compounds represent the first examples of lanthanide complexes intended for studying weak non-covalent interactions to other small molecules in solution.

3. Investigating Weak Interactions by Paramagnetic Tagging of a Lewis Base (Paper I)

3.1 Project Design

Complexes **8** (Lu) and **9** (Dy) were designed and synthesised to characterise weak interactions in dilute solutions. These structures were designed based on the knowledge gained from investigations using two earlier systems that were developed, shown in Figure 12. Using Compound **36**, no binding to strong XB donors was observed where Ln^{3+} was paramagnetic (Dy^{3+}); likely as a result of self-association of pyridine moieties to charged, non-fully-coordinated lanthanide ions. In a different manner, the application of Compound **37** was hindered by its low solubility in polar aprotic solvents.
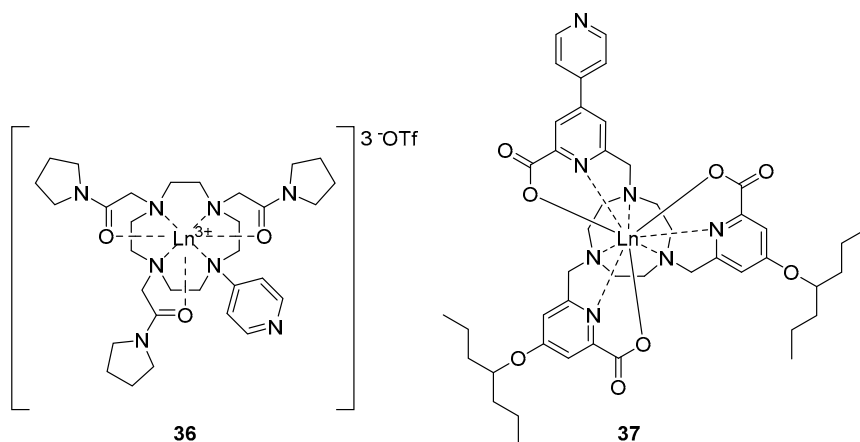

Figure 12. Previous iterations of Lewis basic paramagnetic tag design.

Lewis basic complexes **8** and **9** (Ch. 2.3) were soluble in acetonitrile, and due to the 9-coordination sites provided to the core lanthanide ion, were expected to be suitable for studying their interactions with HB and XB donor systems (Figure 9). In addition, reference systems **45** and **46** were used to exclude that the spectral changes upon addition of HB and XB donors would be due to

dilution or binding by other mechanisms than HB or XB. A 'blank' titration or dilution was also performed to verify this.
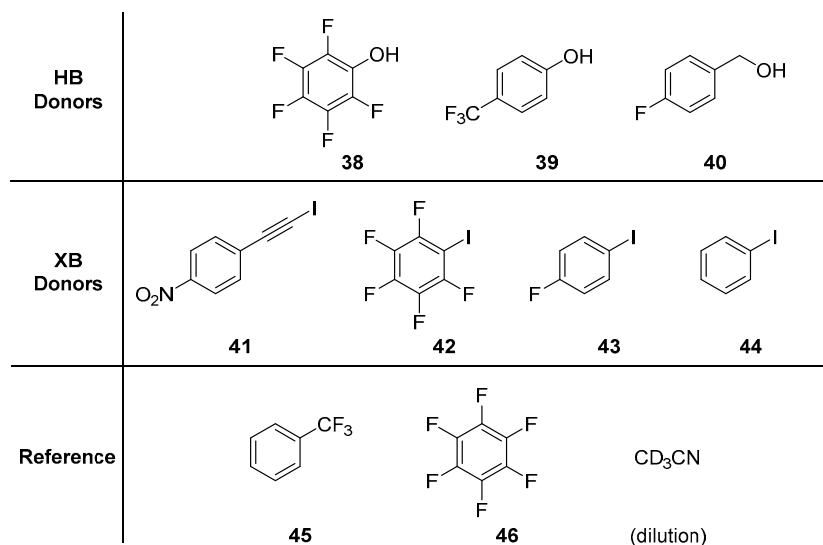

Figure 13. HB donors (**38-40**; top) and XB donors (**41-44**; centre) tested against Compounds **8** and **9**, in decreasing strengths from left to right. Reference compounds (**45** and **46**; bottom) that should elicit no binding were tested, as well as a dilution with *d*-MeCN.
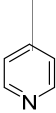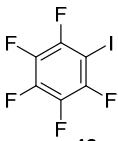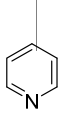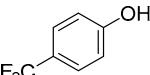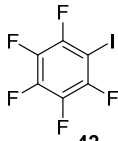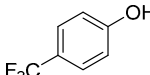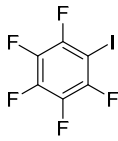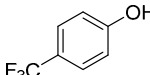
The HB and XB donor interaction partners were selected to provide a series of HB (**38-40**) and XB (**41-44**) donors with varying donor strength, so to detect the limitations of the proposed novel technique. The experiments were performed at a 1.82 mM concentration of host Ln-complex (1.01 mg Compound **8** or 1.00 mg Compound **9** in 500 μL *d*-MeCN), which allowed quick and easy measurement of 1D ^{1}H and ^{19}F NMR spectra. This concentration is close to the current lowest limit used for NMR titration experiments without isotope labelling. It should also be underlined that literature studies of hydrogen/halogen bonding in solution typically study strong interactions at concentrations of 2-100 mM,[12, 55, 73] mostly in more apolar solvents. Hence, the samples studied herein range from comparably strong to much weaker, in polar solvents, and are at least approximately 10 times more diluted. Titration experiments were performed, whereby 0.25, 0.50, 0.75, 1.00, 1.50, 2.00, 5.00, 10.00 and 20.00 equivalents [H] / [G] of guest (G) were added to the NMR tube, and ^{1}H and ^{19}F NMR spectra were recorded.

Reference experiments using α,α,α-trifluorotoluene (**45**) and hexafluorobenzene (**46**) were employed to evaluate whether binding through any other noncovalent interaction, such as π-π interactions, could be detected. Additionally,

dilution experiments were performed to detect and evaluate whether the chemical shifts would be influenced by dilution throughout the course of a titration.

For comparison of the paramagnetic NMR technique with a standard titration, pyridine (**47**) was first titrated with either iodoperfluorobenzene (**42**) or with *p*-trifluoromethylphenol (**39**) at comparable, 1.82 mM concentration. If no interaction takes place between the paramagnetic tag, this experiment is expected to provide comparable chemical shift changes as those obtained for the Lu-complex **8** (Table 2, entry 1). As an additional control, a titration at 1.82 mM host concentration was also performed with these host and guest molecules swapped (Table 2, entry 2). In all cases described, a full NMR titration regime was performed, titrating iodoperfluorobenzene (**42**) or *p*-trifluoromethylphenol (**39**) with pyridine (**47**), with the host and guest being swapped. Next, a titration at a 100 × higher concentration ([host] = 182 mM) was carried out to demonstrate the impact of sample concentration on the detection of weak binding (Table 2, entry 3). In this instance, the host and guest were interchanged, titrating pyridine into iodoperfluorobenzene (**42**) or *p*-trifluoromethylphenol (**39**) solution due to the inability to dissolve the latter in *d*-MeCN at such a high concentration.

Table 2. Control experiments using pyridine (**47**) *versus* iodoperfluorobenzene (**42**) or *p*-trifluoromethylphenol (**39**), to highlight the importance of concentration, and to provide comparison for the performance of the paramagnetic NMR technique developed herein.

Additionally, f2-coupled ^{1}H,^{13}C HSQC spectra were run for all titrations involving lanthanide(III) complexes to attempt to measure RDC's through changes in $^1J_{CH}$ couplings between diamagnetic and paramagnetic samples.

3.2 Results and Discussion

Titrating the paramagnetic Lewis base **9** with HB donors **38**, **39** and **40** resulted in measurable chemical shift changes, significantly larger than the chemical shift changes observed when using the diamagnetic analogue **8**. As an example, the ^{19}F NMR spectra of pentafluorophenol (red), of pentafluorophenol in the presence of 1 eq. diamagnetic Lewis base **8** (green), and of pentafluorophenol and 1 eq. paramagnetic Lewis base **9** (blue) are shown overlaid in Figure 14.
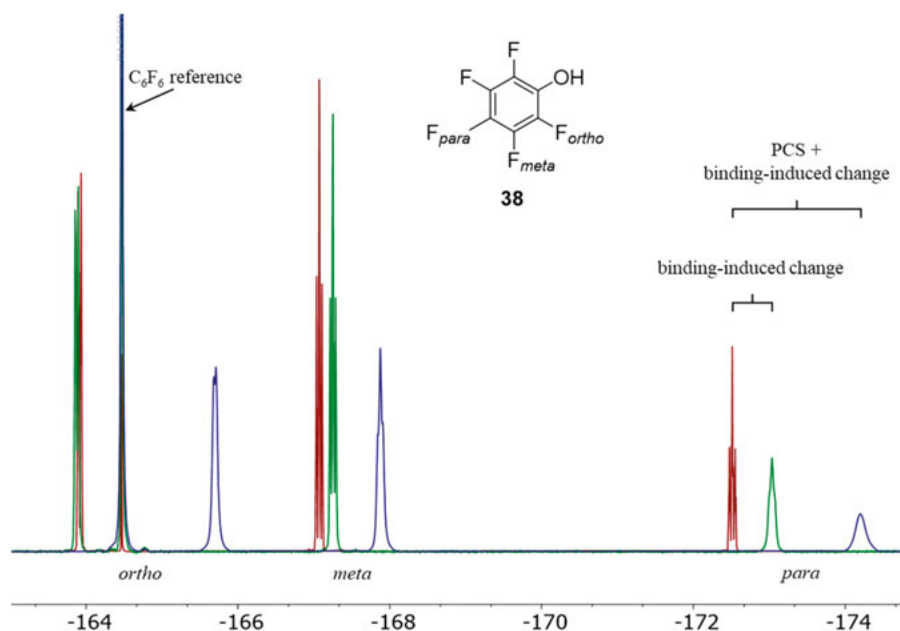

Figure 14. Overlaid spectra of pentafluorophenol **38** (red), pentafluorophenol (**38**) and 1 eq. Lu-complex **8** (green), and pentafluorophenol (**38**) and 1 eq. Dy-complex **9** (blue).

The PCS data was then plotted against the equivalents of HB donor added and non-linear curve fitting was performed using Equation 4.

41

$$y = 1 + \left(\sqrt{^1/_{k_a} + x + C_0 - \left(\left(^1/_{k_a} + x + C_0 \right)^2 - 4 \times C_0 \times x \right)} \right) \times$$
$$\left(^{(y_{lim} - 1)}/_{(2 \times C_0)} \right) \tag{4}$$

where y_{lim} (the y-axis endpoint) is the absolute limit of δ of the HB donor at an infinite excess of it, which was determined by a separate measurement of its chemical shift at an arbitrary 40 equivalents' concentration as compared to the Lewis base. K_a is the association constant determined for each signal over the titration range, and C_0 is the initial concentration of the host (Compound **8** or **9**). Values of PCS were normalised to begin at a value of 1, so to allow easy comparisons to be made.

Based on the above analysis, $K_a = 2.4$ M^{-1} was deduced using PCS's calculated for the interaction of Lewis bases **8** (diamagnetic) and **9** (paramagnetic) with pentafluorophenol **38**, whereas $K_a = 0.6$ M^{-1} was found for 4-trifluoro-methylphenol **39** (Figure 15) in the same way. These association constants are in reasonable agreement with the literature.[55] In order to explore the scope and limitations of this technique, 4-fluorobenzyl alcohol **40** was tested in the same way. Whereas a binding curve could be detected, a reliable K_a could not be determined due to the binding being too weak, producing too shallow a curve to be quantifiable.
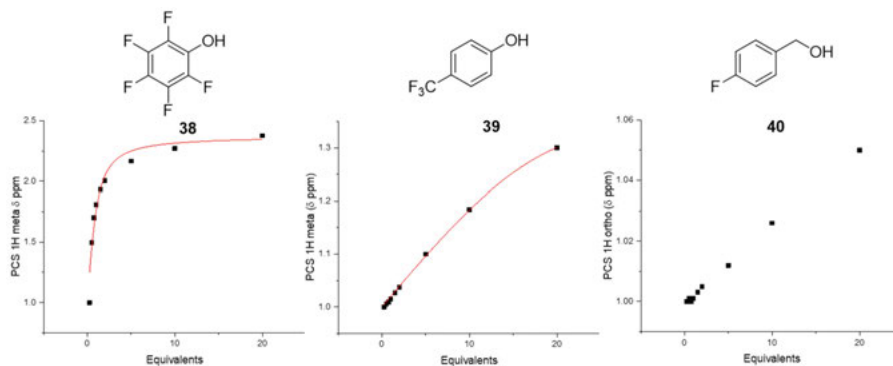
Figure 15. Binding curves of PCS (y-axis) against equivalents of [H] / [G] (x-axis), for pentafluorophenol **38** (left), 4-trifluoromethylphenol **39** (centre) and 4-fluoroben-zyl alcohol **40** (right) over a titration with Lewis basic complexes **8** (diamagnetic) and **9** (paramagnetic).

It should be underlined that titrating pyridine (**47**) at the same concentration, 1.82 mM, in an analogous manner to that described above for the paramag-

netic lanthanide tagged pyridine (**9**), with 4-trifluoromethylphenol (**39**) provided no binding induced chemical shift changes (Figure 16). In agreement with expectations, the titration of the diamagnetic Lu-complex (**8**) with 4-trifluoromethylphenol (**39**), at the same concentration, gave comparably small chemical shift changes to those observed for the titration of pyridine, yielding extremely shallow binding curves at best. This confirms that the lanthanide tag, when diamagnetic, does not significantly alter the Lewis basicity of the attached pyridine.
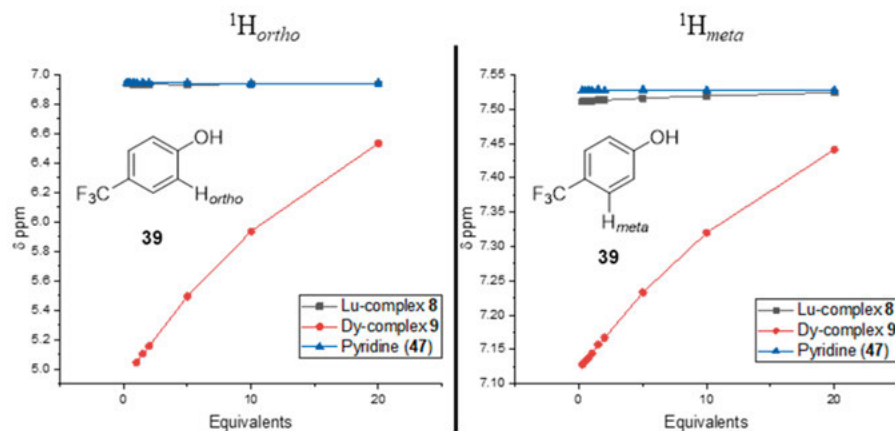
Figure 16. Comparison of 4-trifluoromethylphenol (**39**) binding with [1.82 mM] pyridine (**47**; blue), diamagnetic Lu-complex **8** (black) and paramagnetic Dy-complex **9** (red) Lewis basic hosts for aromatic ^{1}H signals *ortho* (left) and *meta* (right) to the interacting hydroxyl group on **39**.

To demonstrate the influence of concentration on determination of association constants, the K_a of pyridine and 4-trifluoromethylphenol was determined at 100 times higher concentration, at 182 mM. Due to the limited solubility of *p*-trifluoromethylphenol in acetonitrile, the interaction partners were interchanged for this titration. Hence, 4-trifluoromethylphenol [182 mM] was titrated with pyridine [6.065 M], which provided quantifiable chemical shift changes (Figure 17) yielding K_a = ~3 M^{-1} for both the pyridine and the phenol. For further reference, a titration using 4-trifluoromethylphenol at 1.82 mM, was carried out. This titration, alike those involving Lu-complex **8** or with host and guest switched, showed no significant Δδ as expected.
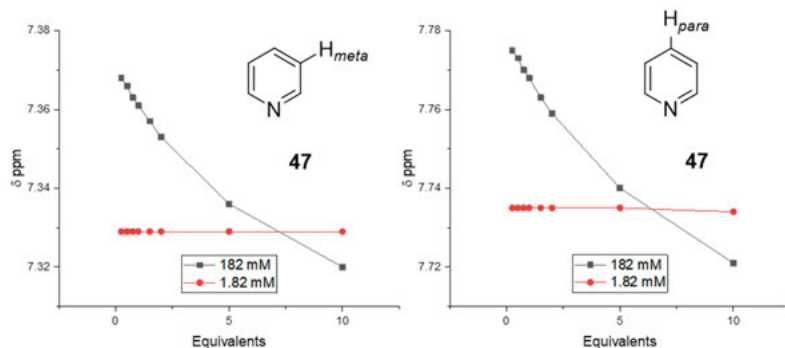
Figure 17. Effect of concentration on a titration. A 4-trifluoromethylphenol HB donor host at 1.82 mM and 182 mM concentrations is titrated with pyridine in relative equivalents.

Overall, the above experiments indicate that by detection of PCS's, instead of binding induced chemical shift changes, the association constants of a non-covalent interaction can be determined at a ≫6 times lower concentration. This is unprecedented.

Throughout the titration of the paramagnetic Lewis base complex **9** with phenols, the phenolic proton showed a chemical shift increase in an opposite direction to those of the C-H protons. This chemical shift change opposes also the direction of change for the corresponding diamagnetic complex **8**. This observation indicates that the PCS observed at this proton is of opposite sign as compared to those observed for the C-H protons, and that its magnitude is much larger than the binding induced chemical shift change itself. Remarkably, upon hydrogen bonding, the proton involved is deshielded, resulting in a higher chemical shift – as seen upon addition to a diamagnetic Lewis base host. Upon more addition of a HB donor, more uncomplexed HB donor exists, pushing the fast-exchanging average signal closer towards its uncomplexed value. The result of the chemical shift approaching from opposite, lower chemical shifts, is likely a result of it being influenced by a different isosurface to the rest of the molecule. Due to this, and to extensive broadening, K_a values could not be determined.

In order to explore whether complexation induced RDC's can be detected – which would be indicative of the partial orientation of the diamagnetic Lewis acid upon interaction with the paramagnetic Lewis base – an f2-coupled ^{1}H,^{13}C HSQC was measured for the complex of 4-trifluoromethylphenol with the paramagnetic Lewis base **9** and for the diamagnetic one, **8**, with the Lewis

basic and Lewis acidic components being in a 1:1.5 concentration ratio (Figure 18). RDC's were calculated as the difference of the $^1J_{CH}$ measured in the two solutions, with **8** and **9**. It should be emphasised that this is the very first report of detection of RDC's upon transfer of orientation of a paramagnetic species to a diamagnetic one via a single, weak non-covalent force. Due to a lack of independent vectors, this preliminary observation merely provides the basis of future geometric characterisation in solution using RDC's.
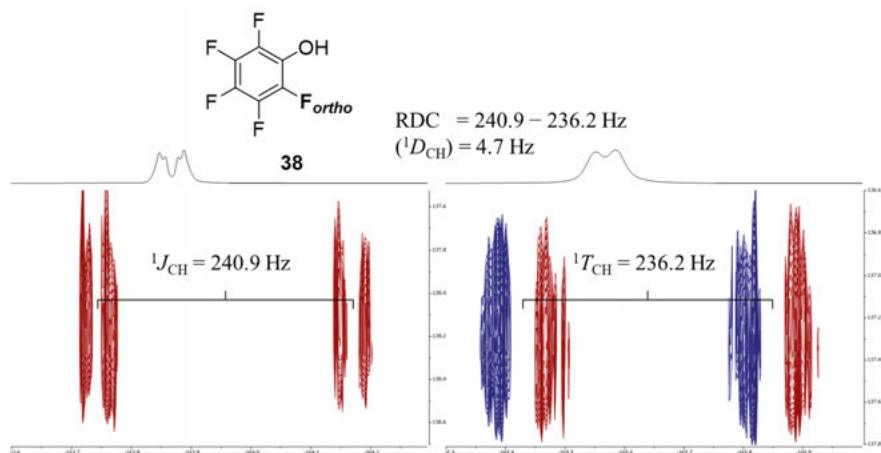
Figure 18. f2-coupled HSQC spectra of pentafluorophenol HB donor (**38**) with the diamagnetic complex **8** (Lu; left) and paramagnetic complex **9** (Dy; right), showing $^1J_{CH}$ and $^1T_{CH}$ couplings, and a deduced RDC ($^1D_{CH}$) for the $^{19}F_{ortho}$ signal.

Throughout titration of a non-interacting species, α,α,α-trifluorotoluene (**45**), with Dy-complex **9**, no significant $\Delta\delta^1H$ could be observed. This supports our findings that the lanthanide complex binds through its Lewis basic pyridine moiety.

In the above experiments, a drift of all ^1H NMR signals was observed for the solutions that contain a paramagnetic complex. This change is not observable when the solvent residual signal is used as a reference, but becomes measurable when employing an internal reference containing *d*-DMSO immersed in the solution in a capillary. This is of significance as most literature studies that report PCS data use the solvent residual signal as a chemical shift reference. In our hands, the PCS's detected in this manner have a large measurement error due to the chemical shift drift. For correction of this error, the drift can be quantified and deduced from the data by measuring this chemical shift drift on the solvent signal upon dilution in titration steps using the solvent as the titrant, in equal steps, in a separate experiment. Alternatively, the true drift independent PCS's can be deduced as the difference of the chemical shift

change of a signal of the diamagnetic component (PCS + drift) and of the chemical shift change of the solvent residual signal (drift). For ^{1}H measurements, referencing to the residual d-MeCN solvent peak as opposed to the capillary-contained d-DMSO peak effectively cancelled out this drift effect.

Titrations probing halogen bonding were also performed with Lewis basic lanthanide(III) complexes **8** and **9** against XB donors **41**, **42**, **43** and **44**, as well as **46** (Figure 13). Subtracting the linearly-dependent drift of various fluorinated reference compounds contained in the reference capillary d-DMSO solution, as explained above, gave shallow, weak binding curves that were determined *via* PCS's. Due to the weak nature of these, no K_a could be determined, which was not unexpected given that the K_a values expected were less than 1.[55, 73] Nevertheless, the magnitude of the PCS is reliant on the propensity of the XB donor to form XB's, indicating that halogen bonding could be detected at low concentrations *via* this new strategy.

3.3   Concluding Remarks

A new paramagnetic NMR technique was introduced for the detection and quantification of weak non-covalent interactions in solution. This new method was demonstrated to be capable of determining the binding constant of hydrogen bond complexes with $K_a \geq 2.4$ mM at $\gg$6 times lower concentration than with standard NMR titration experiments. Hydrogen bonds as weak as $K_a \sim$ 0.6 mM that are undetectable at this concentration by standard NMR titration were shown to be detectable, even if not reliably quantifiable in terms of K_a. Thus, this work has laid the foundations for a novel NMR technique that allows the detection and analysis of weak complexes at concentrations that are not possible with the current standard NMR techniques. The key feature of this new technique is the detection of PCS's that are transferred from a paramagnetic to a diamagnetic component via a weak interaction force, rather than detecting binding induced chemical shift changes.

4. Investigating Weak Interactions by Paramagnetic Tagging of a Lewis Acid (Paper II)

4.1 Project Design

Complexes **10** (Lu) and **11** (Dy) (Figure 10) were designed to characterise a non-covalent bond – in this case halogen bonding – in dilute solution. As a complement to the studies discussed in Chapter 3, a Lewis acidic halogen bond donor was attached to a Ln-complex and was titrated against the Lewis bases (XB acceptors) 1-methyl-1H-pyrrolo[3,2-b]pyridine (**48**) and strychnine (**49**) (Figure 19).

48   **49**
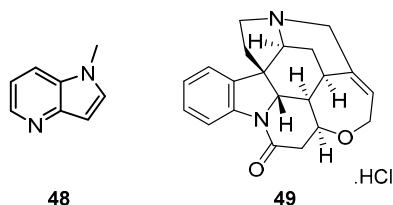
Figure 19. Lewis bases, 1-methyl-1H-pyrrolo[3,2-b]pyridine **48** and strychnine **49**, tested against XB donor Ln(III) complexes **10** and **11**.

These Lewis bases were expected to be optimal for model studies as they are rigid, non-protic, non-competitive, their pK_a is in the range of 7-9 and hence their Lewis basic interaction site can easily be held in a deprotonated form, and they contain ≥ 5 independent C-H bond vectors which is required for determination of the geometry of their Lewis acid bound complex. 1-methyl-1H-pyrrolo[3,2-b]pyridine (**48**) has the advantage of being structurally simple, while strychnine (**49**) is a complex molecule that is often used in NMR methodology development.[142, 143, 144]

4.2 Results and Discussion

The halogen bond donor complexes **10** (Lu) and **11** (Dy) were titrated with Lewis bases 1-methyl-1H-pyrrolo[3,2-b]pyridine (**48**) and strychnine (**49**) using ^{1}H,^{13}C HSQC experiments for detection. The PCS's observable on the diamagnetic Lewis bases were determined by calculating the chemical shift difference of the corresponding NMR peaks of the paramagnetic and diamagnetic samples at each titration point. In addition to PCS's, PRE was acquired for the Lewis base by calculating the difference of the half-line-width of the samples containing the paramagnetic and the corresponding diamagnetic Lewis acids. Although HSQC spectra were obtained to circumvent signal overlap, ^{1}H traces were used for chemical shift determination (for PCS and PRE measurements); ^{13}C NMR data was too noisy to be reliably used due to low resolution. RDC's were determined by acquiring f2-coupled ^{1}H,^{13}C HSQC spectra and calculating the difference of the $^1J_{CH}$ for the samples containing a paramagnetic or a diamagnetic lanthanide ion.

The PCS's of 1-methyl-1H-pyrrolo[3,2-b]pyridine (**48**) were plotted as a function of their concentration in solution (Figure 20). The binding constant was determined to $K_a = 2.29$ M^{-1} by analysis of the binding curve of the signal of the proton *ortho* to the interacting Lewis basic nitrogen (red, Figure 20) with the binding Equation 4. This K_a agrees well with the association constants of analogous systems reported in the literature.[73]
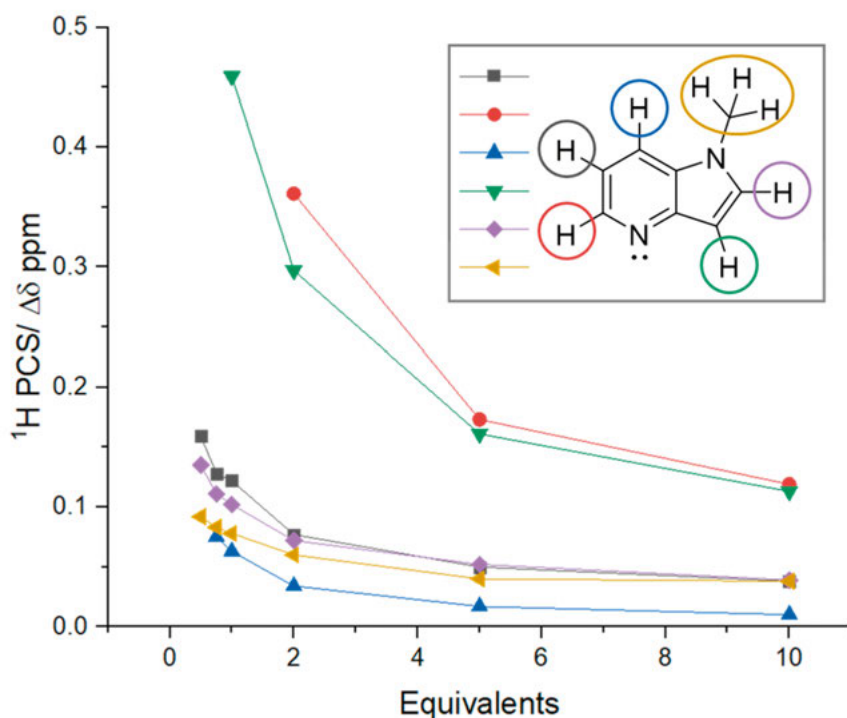
Figure 20. ^{1}H NMR titration data showing PCS calculated from titration with XB donors **10** and **11** *versus* Lewis base **48**.

'Paramagpy' and 'MSpin' software were used to analyse the PCS, RDC and PRE data in terms of molecular geometry. Here, the NMR data acquired at a concentration ratio [diamagnetic Lewis base] : [paramagnetic Lewis acid] = 1.5 : 1 was used, as spectra at lower diamagnetic/paramagnetic ratios suffered from signal broadening, whereas at higher ratios were expected to contain less of the oriented diamagnetic component.

In order to identify the geometry of the halogen bond complex that best fits the experimental data–containing PCS's and RDC's–an ensemble of geometries with different I···N distances, with various Ln-I···N tilt angles (varied in 15° increments) and a variety of rotations around the C-I···N bond (varied in 15° steps) were prepared in MSpin software. The geometry shown in Figure 21 possessing a XB length of 2.990 Å (85 % of the sum of the van der Waal's radii of I and N) at 0 ° rotation and 0 ° tilt provided the best fit. Validation of these results was then carried out by back-calculating values with Paramagpy software to give a combined, overall Q-factor of 0.2634, including PRE, PCS

and RDC components. A Q-factor <0.3 is usually considered as a good fitting. It should be underlined that the identified bond geometry agrees well with our expectations (bond length ~ $\sum$vdW radii of the participating atoms, 180 ° and C-I$\cdots$N bond angle).
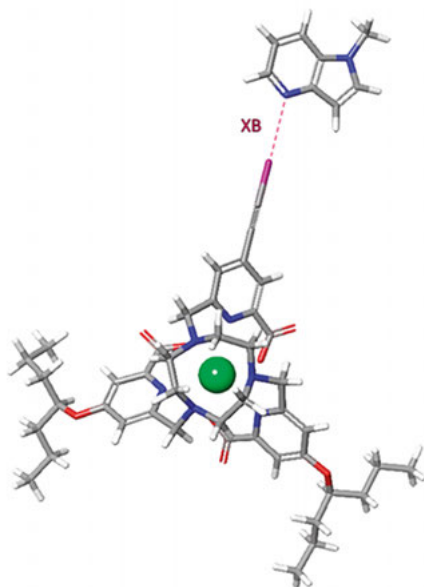
Figure 21. The geometry best fitting to the experimental PCS and RDC data for the XB complex between Ln-tag **11** and Lewis base **48**.

Reference measurements, titrating the Lewis base **48** with trialkylated (**50**) and acetylene-functionalised (**35**) Dy^{3+} complexes (Figure 22) showed no significant change in chemical shift throughout the titration. This is further proof that the interaction seen is truly through the halogen bond, and not to the central lanthanide metal itself.
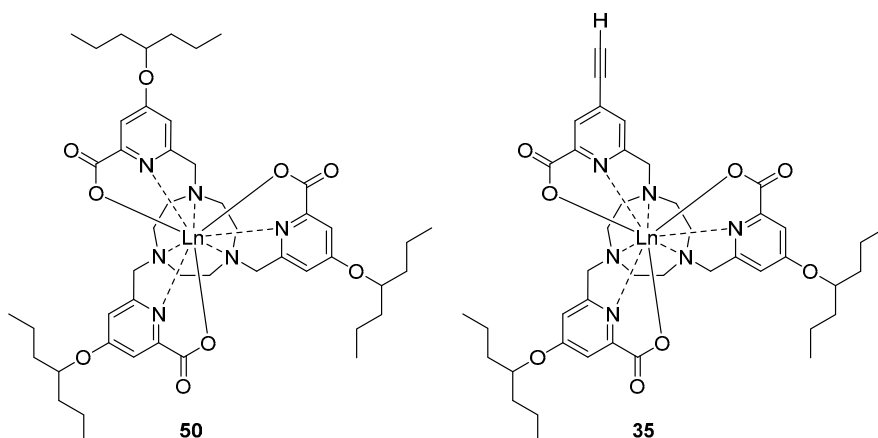
Figure 22. Trialkylated (**50**) and acetylene-functionalised (**35**) Dy^{3+} complexes as reference compounds.

Whereas 1-methyl-1H-pyrrolo[3,2-b]pyridine (**48**) was an optimal Lewis base for a first initial study, it is planar and has a low number of C-H bonds. We therefore performed analogous measurements titrating the halogen bond donor complexes **10** (Lu) and **11** (Dy) with strychnine (**49**). The latter has a larger number of nuclei on which RDC's, PCS's and PRE can be detected, is rigid so reduces the possible number of conformers (simplifying its analysis), possesses a geometry with C-H bond vectors in more diverse orientations, and is a complex natural product in contrast to **48** that is a vastly simplified model compound.

PCS's were detected on protons adjacent to the interacting Lewis basic nitrogen, providing proof of a halogen bonding interaction, yet these values exhibited large errors when binding constants were determined with Eq. 4; hence, they could not be determined.

As the PRE and RDC's obtained at the concentration ratio of [strychnine] : [paramagnetic XB donor] = 1.5 : 1 were also of comparable magnitude as the associated experimental error, the RDC data was not analysed further in terms of 3D molecular structure. This was mainly due to limitations of CD$_3$CN solubility; CD$_2$Cl$_2$ solution was thus used instead, with both interacting partners still being dissolved at lower concentrations than previously. Furthermore, Strychnine is known to react with CD$_2$Cl$_2$ over time,[145] meaning that longer data acquisition times were not possible and no further attempts at data acquisition were performed.

4.3 Concluding Remarks

As a complement to the studies presented in Chapter 3, a paramagnetically labelled halogen bond donor (Lewis acid) was synthesised and its interaction with two Lewis bases was studied in acetonitrile and dichloromethane solutions, respectively. When placed into a strong magnetic field, the orientation of the diamagnetic Lewis base *via* a halogen bond to the paramagnetic Lewis acid was observed. Based on PCS and RDC data observed for the diamagnetic Lewis base, the association constant and the bound geometry was identified for the interaction of a simple model system, **48** (halogen bond acceptor), and an iodoacetylene, **11** (halogen bond donor). The PRE observed on each signal provided less useful data for the description of the geometry of the complex than the RDC's and PCS's, yet helped refinement of the overall fitting. Analysis of the interaction of strychnine (**49**) with the paramagnetically labelled halogen bond donor (**11**) allowed the observation of PCS's yet without reliable quantification of association constants. Analysis based on RDC's and PRE did not provide a reliable geometry due to extensive line-broadening of the NMR signals of strychnine, low solubility and reactivity with CD_2Cl_2. This data provides the first evidence that a single weak interaction force, a halogen bond, can be studied by paramagnetic tagging of a Lewis acid (halogen bond donor) and detecting paramagnetism-affected NMR observables on the diamagnetic interaction partner Lewis base (halogen bond acceptor). Analysis of the PCS's observed on the diamagnetic interaction partner was demonstrated to allow the determination of the association constant of the interaction, and also the determination of the geometry of the XB complex in solution. The analysis has been performed at a host concentration as low as 2.20 mM in solution, which is around 30 times lower than that used in standard NMR titrations with comparable systems.[73]

5. Investigating Nucleophilic Iodonium Interactions in Solution (Paper III)

5.1 Nucleophilic Iodonium Interactions (NII's)

NII's were proposed by Rissanen *et al* in early 2021 and gathered a lot of attention[7, 8, 146, 147] as an remarkable, attractive interaction between cationic silver(I) and cationic iodine(I) complexes (Figure 23) . They were proposed based on X-ray, computational, ITC and NMR data, and iodine(I) was proposed to act as nucleophile by donating electrons from a filled p-orbital into an empty d-orbital of the analogous silver(I) complex. The proposed, unexpectedly high bond strength of 113 kJ/mol was anomalous, along with unsystematic chemical shift changes proposed upon formation of NII complexes with various electron donor and acceptor substituents. We therefore decided to re-examine this system in solution.
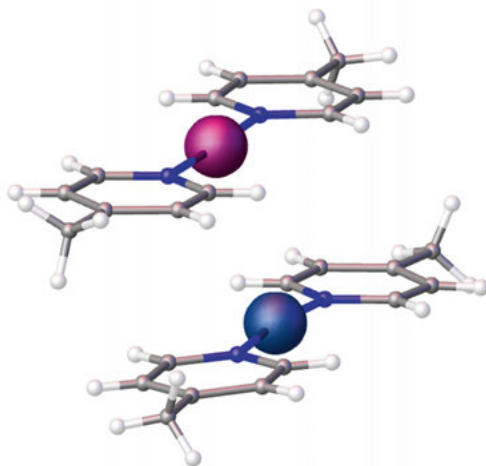

Figure 23. Crystal structure incorporating a proposed NII. The offset between aromatic rings suggests a π-π interaction.

5.2 Silver (I) and Iodine (I) Complexes and their Synthesis

Silver(I) possesses up to six coordination sites,[148, 149] and forms weak coordinative complexes. The iodine(I) of "iodonium" complexes forms 3c4e halogen bonds through coordination of two Lewis bases via their p-hole. Iodine(I) can only coordinate to two Lewis basic ligands, creating an exceedingly strong (up to 180 kJ/mol) halogen bond, particularly when nitrogen-based Lewis bases are used.[150] These halogen bonds prefer a symmetric geometry, and iodine(I) complexes are applicable as electrophilic halogen transfer reagents.[151]

[Bis(pyridine)silver(I)]+ complexes were prepared by mixing a silver salt with two equivalents of pyridine (Scheme 7). To access the analogous iodine(I) complexes, the silver(I) complex can react with I_2 in a dry, mildly polar solvent.[152] The reaction is driven by the formation of AgI that forms a yellow precipitate in CH_2Cl_2. The iodine(I) formed in this reaction is stabilised by two coordinating Lewis bases, typically the ligands of the original silver(I) complex. The synthesis of [bis(pyridine)iodine(I)]+-type complexes (Scheme 7)[153] looks straightforward, but instead requires meticulous preparation under inert, anhydrous conditions – easiest to achieve in a glovebox. Halogen(I) complexes are moisture sensitive and hydrolyse rapidly under ambient (moist) conditions.[152]
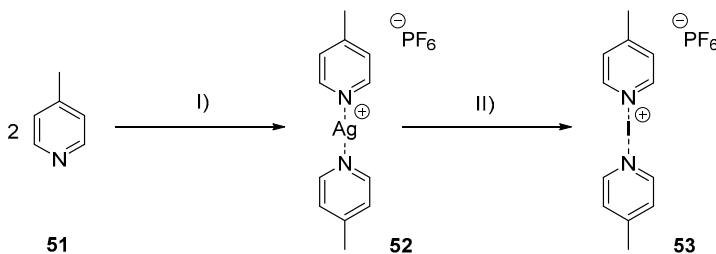
Scheme 7. Synthesis of [bis(4-methylpyridine)silver(I)]+ and [bis(4-methylpyridine)iodine(I)]+ complexes, with associated hexafluorophosphate anions. *I) 4-picoline (2.0 equiv.), AgPF₆ (1.0 eq.), CH₂Cl₂, rt, 5 min, 98%; II) I₂ (1.05 eq.), CH₂Cl₂, rt, 30 min, 85%.*

Synthesis of [bis(4-methylpyridine)iodine(I)]+ (Scheme 7) proceeded by first complexing *(I)* 2 equivalents of 4-picoline (**51**) with AgPF₆. The resulting complex was precipitated with *n*-hexane, centrifuged and dried to afford **52** as a white powder. **52** was then treated with I₂, carrying out halonium ion transfer *(II)* and causing AgI to precipitate as a yellow solid. The iodonium complex,

53, was obtained by removal of AgI, then precipitation with *n*-hexane, centrifugation, drying, washing with *n*-hexane and repeating, to give **53** as a white, crystalline solid.

A [bis(pyridine)iodine(I)]$^+$ complex that disfavours ligand (pyridine) exchange, achieved by using a bidentate backbone, was also synthesised (Scheme 8) in an analogous manner to that shown above.[153]
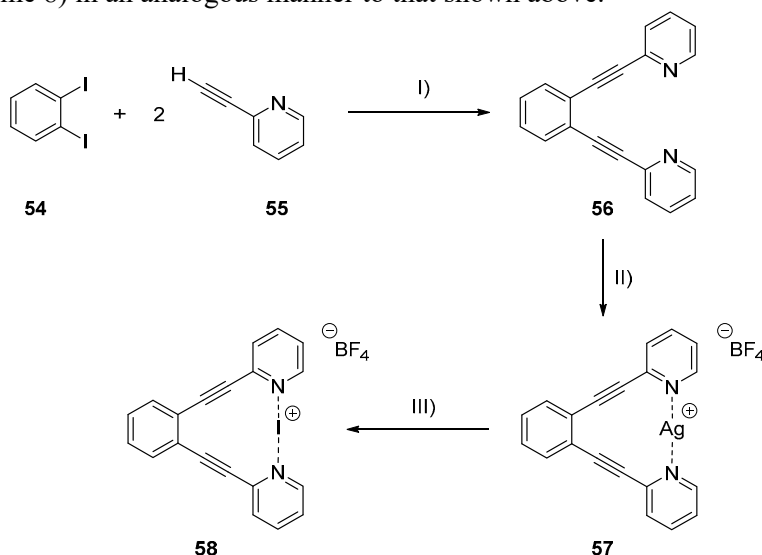
Scheme 8. Synthesis of 1,2-bis[((pyridine-2-ylethynyl)-benzene)silver(I)]$^+$ and 1,2-bis[((pyridine-2-ylethynyl)-benzene)iodine(I)]$^+$ complexes as their tetrafluoroborate salts. *I) 1,2-diiodobenzene (1.0 eq.), 2-ethynylpyridine (2.3 eq.), PdPPh$_3$Cl$_2$ (10 mol%), CuI (11 mol%), DEA/DMF 3:1, N$_2$, µW 120 °C, 10 min, 68%; II) AgBF$_4$ (1.0 eq.), CH$_2$Cl$_2$, rt, 10 min, 87%; III) I$_2$ (1.05 eq.), CH$_2$Cl$_2$, rt, 30 min, 98%.*

To synthesise these bidentate complexes (Scheme 8), a double Sonogashira cross-coupling reaction *(I)* was first carried out, with 1,2-diiodobenzene (**54**) and 4-ethynylpyridine (**55**). After filtration, extraction and two rounds of silica gel chromatography to afford **56**, Ag$^+$ complexation *(II)* was achieved by introduction of AgBF$_4$ to a solution of **56** in CH$_2$Cl$_2$. The silver(I) complex (**57**) was then precipitated with *n*-hexane, centrifuged and dried to afford a white powder. Following this, **58** was attained by halonium ion transfer *(III)* of **57** with I$_2$ in CH$_2$Cl$_2$. Formation of a yellow AgI precipitate and a faint purple colour (indicating a slight excess of I$_2$) indicated completion. Removal of **58** from solid AgI, precipitation of the iodine(I) complex with *n*-hexane, centrifugation, drying, and a further washing procedure yielded **58** as a white, crystalline solid.

The silver(I) and iodine(I) complexes were characterised using ^{1}H,^{15}N HMBC NMR experiments. [Bis(pyridine)silver(I)]$^+$ (**52**) was identified by its δ^{15}N = -131 ppm, whereas the[bis(pyridine)iodine(I)]$^+$ complex (**53**) was identified based on its characteristic δ^{15}N = -181 ppm.[78]

5.3 An NMR-based Insight into the (Non-) Existence of NII's

To re-evaluate the structure of the complexes studied by Rissanen and coworkers,[7] bis(4-methylpyridine)silver(I)]$^+$ (**52**) and [bis(4-methylpyri-dine)iodine(I)]$^+$ (**53**) complexes with PF$_6^-$ counterions were freshly synthe-sised (Scheme 7) under inert, dry conditions. The two complexes were mixed at varying molar ratios in CD$_2$Cl$_2$, and studied using ^{1}H NMR, ^{1}H,^{15}N HMBC and ^{1}H/^{19}F DOSY experiments.

The ^{1}H and ^{19}F NMR spectra of pure bis(4-methylpyridine)silver(I)]$^+$ (**52**) and [bis(4-methylpyridine)iodine(I)]$^+$ (**53**) samples, and of their 3:1, 2:2 and 1:3 mixtures were recorded. The mixing of the silver(I) and iodine(I) complexes resulted in insignificant-to-no changes of the ^{1}H and ^{19}F NMR chemical shifts of the two complexes. This is unexpected, assuming that a >100 kJ/mol inter-action between the complexes takes place. ^{1}H,^{15}N HMBC experiments on the mixtures showed two distinct sets of cross-peaks – one for each species. The mixing of the two complexes showed small ^{15}N chemical shift changes for the nitrogens of the silver(I) species (**52**), whereas no change for the iodine(I) species (**53**), within experimental error, was observed (Table 3). ^{1}H and ^{19}F DOSY spectra acquired for the mixtures showed neither significant variation of the diffusion coefficients upon mixing the complexes, nor upon alteration of the concentration ratios. Upon interaction of the silver(I) and iodine(I) com-plexes, a decrease of the diffusion coefficients of both complexes would have been expected; this was not observed (Table 3).

Table 3. Results of ^{1}H,^{15}N HMBC and ^{1}H DOSY experiments,

Mixture	δ^{15}N (ppm)		$D \times 10^{-10}$ m s^{-2}	
53 (I) / 52 (Ag)	53 (I)	52 (Ag)	53 (I)	52 (Ag)
4 : 0	-181.0	–	11.8	–
3 : 1	-181.1	-131.2	11.9	12.0
2 : 2	-181.0	-130.4	12.1	11.8
1 : 3	-181.1	-130.8	11.8	11.5
0 : 4	–	-130.8	–	11.6

[Bis(pyridine)halogen(I)]$^+$ and [bis(pyridine)silver(I)]$^+$ complexes are highly dynamic in nature, and exist as a mixture of their associated and dissociated forms.[154] When both silver(I) and iodine(I) complexes (**52** and **53**) are introduced to one another in solution, ligand scrambling takes place.[154] This was confirmed by ^{1}H,^{1}H NOESY, where clear exchange (EXSY) cross-peaks were observed (Figure 24).

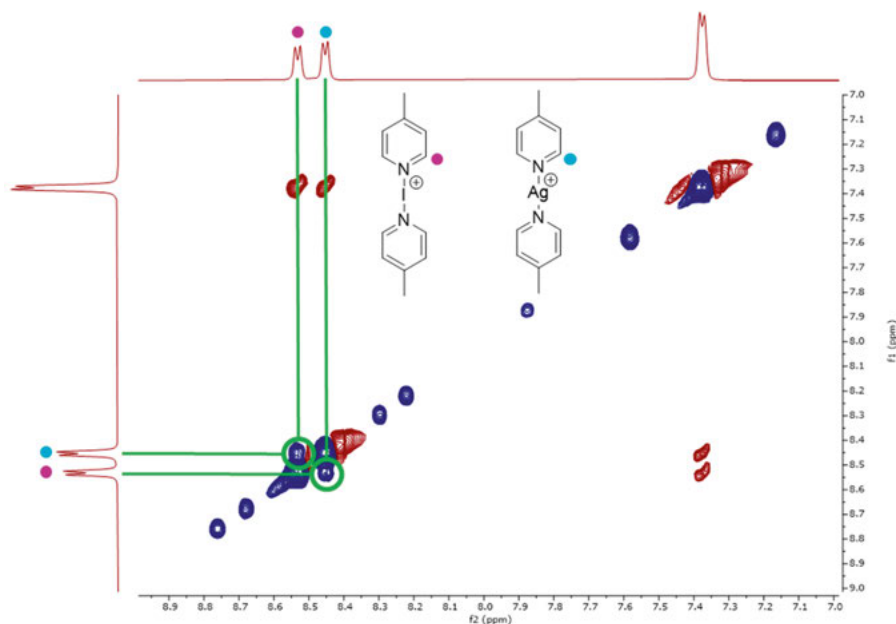Figure 24. NOESY spectrum of a 1:1 mixture of [bis(4-methylpyridine)iodine(I)]$^+$ (**53**) and [bis(4-methylpyridine)silver(I)]$^+$ (**52**). EXSY cross-peaks (blue) between the two complexes are highlighted.

As there was no sign of ^{1}H,^{15}N chemical shift changes upon mixing the silver(I) and iodine(I) complexes (**52** and **53**) that would be comparable to those originally reported, we tainted samples with various common contaminants. Adding water to the silver(I) complex (**52**) resulted in no significant $\Delta\delta^{15}$N. This corroborated a previous study showing that coordination of oxygen ligands does not elicit a large $\Delta\delta$.[150] Addition of increasing amounts of 4-picoline (**51**) increased the δ^{15}N. This is best explained by silver(I) coordinating a third 4-picoline, and the 4-picoline being in a dynamic equilibrium with 4-picoline free in solution (δ^{15}N = -71.6 ppm) which is expected to result in deshielding of the population-averaged nitrogen NMR signal. Upon addition of trifluoroacetic acid (TFA) or of 4-picoline-H$^+$, the δ^{15}N decreased dramatically, tending towards the native δ^{15}N of 4-picoline-H$^+$ (-173.3 ppm). Adding water to a sample of the I$^+$ complex (**53**) resulted in an unchanged δ^{15}N of the complex, but with a new signal of 4-picoline-H$^+$ appearing. This suggests the acid induced partial decomposition of the iodine(I) complex, the release of hypoiodous acid and slow exchange of 4-picoline (on the NMR timescale) between the iodine(I) and proton complexes. Water was added to a mixture of the iodine(I) and silver(I) complexes and resulted in no change of the δ^{15}N of the [bis(4-methylpyridine)iodine(I)]$^+$ (**53**) complex, whereas a measurable negative $\Delta\delta^{15}$N of the [bis(4-methylpyridine)silver(I)]$^+$ (**52**) complex was observed. This can be explained by moisture induced release of 4-picoline from the [bis(4-methylpyridine)iodine(I)]$^+$ (**53**) complex along with hypoiodous acid in trace amounts. The resulting protonated 4-picoline-H$^+$ enters into quick ligand exchange with the [bis(4-methylpyridine)silver(I)]$^+$ (**52**) complex, yielding a time-averaged NMR signal that is strongly shifted towards the more populated [bis(4-methylpyridine)silver(I)]$^+$ (**52**) complex, yet is affected by the chemical shift of the 4-picoline-H$^+$ ion (δ^{15}N = -173.3 ppm) (Figure 25). The observation of a small $\Delta\delta^{15}$N upon mixing iodine(I) and silver(I) complexes in the original report of Rissanen *et al*, which do not show any systematic electron density dependence, may thus be explained by a varying amount of moisture in the samples.
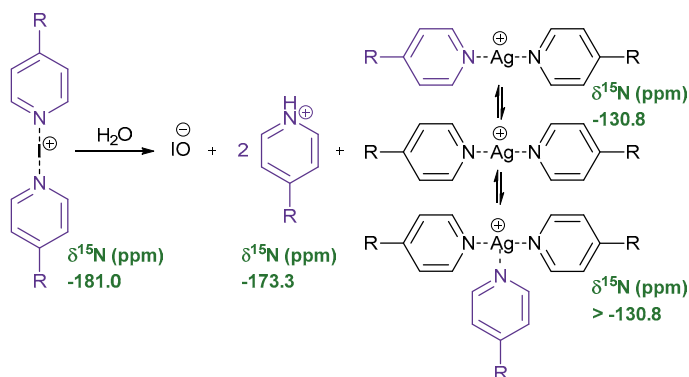
Figure 25. Equilibrium process between [bis(4-methylpyridine)iodine(I)]⁺ (**53**) decomposition products and a changing $\delta^{15}N$ of [bis(4-methylpyridine)silver(I)]⁺ (**52**) in CD₂Cl₂.

To omit the possibility that the above conclusion was influenced by a fast exchange processes between the iodine(I) and silver(I) complexes (**52** and **53**), bidentate 1,2-bis[((pyridine-2-ylethynyl)-benzene)silver(I)]⁺ (**57**) and 1,2-bis[((pyridine-2-ylethynyl)-benzene)iodine(I)]⁺ (**58**) complexes and their mixtures were studied (Scheme 8). The ¹H,¹H NOESY spectrum obtained for the mixture, with a mixing time of 1 s, contained no EXSY crosspeaks between the silver(I) and iodine(I) complexes, confirming that there is no ligand exchange between the two complexes. In a similar fashion to the study of the 4-picoline complexes above, mixtures of each of the two species were made, and ¹H,¹⁵N HMBC and ¹H DOSY experiments were run. No sign of interaction between the two complexes was observed, hence no $\Delta\delta^{15}N$ or alteration of the diffusion coefficients were seen upon mixing or varying the concentration ratios of the two complexes.

The DFT calculations originally published by Rissanen *et al* were redone with a series of different basis sets to evaluate the interaction of [bis(4-methylpyridine)silver(I)]⁺ (**52**) and [bis(4-methylpyridine)iodine(I)]⁺ (**53**) complexes to ensure that any interaction, or lack of interaction, does not originate from an arbitrarily chosen computational method itself.[155] The X-ray structure of the iodine(I) and silver(I) complex shown in Figure 23 was used as the starting point for the calculations. These calculations showed that, independent of the chosen method, a very weak interaction energy (-6.5 to -14 kcal/mol, Table 2, Paper III) is expected to be countered by the entropy and thermal energy at room temperature, rendering the interaction insignificant in solution. Calculations also showed that the main attractive force between the two complexes was the π-π interaction between aromatic rings, whereas the silver(I)–iodine(I)

contact itself is endothermic and is therefore dominated by Coulomb repulsion. Hence, the computations indicate that there is no attractive force between silver(I) and iodine(I), and if there is any attraction between their bis(pyridine) complexes, this must be due to a π-π interaction between their aromatic rings. However, even this is too weak to be measurable in solution.

Whereas we performed no X-ray analysis, it should be considered that close contacts observed in a crystal structure do not necessarily indicate an attractive interaction. The X-ray structure CSD EROGIE suggests π-π interaction of the aromatic rings, yet this does not prove an iodine(I)–silver(I) attractive force. The close contact of the two complexes is likely made possible by the extensive charge transfer[156] within the silver(I) and within the iodine(I) complexes. Such close contacts have previously been seen between two iodine(I) ions when encompassed into a helical structure;[156] this is not a sign of an iodine(I)-iodine(I) attractive force but can rather be interpreted as the result of charge transfer minimising repulsion, along with the complexing nitrogen ligand promoting a close contact.

5.4 Concluding Remarks

NMR spectroscopic reinvestigation of the recently proposed nucleophilic iodonium interaction (NII) in solution provided no evidence for the existence of this interaction. Ligand exchange between iodine(I) and silver(I) complexes was detected, and the previously published unsystematic changes in NMR parameters upon mixing the two complexes was explained for most samples with a varying amount of water content. Overall, the finding that there is no evidence for the formation of NII's in solution emphasises the need for a critical application of spectroscopic techniques when studying weak non-covalent forces. Working at the very limits of current techniques increases the risk of data over-interpretation and reflects the need for the development of more sensitive methodologies.

6. Concluding Remarks and Perspective

This thesis takes a deeper look into characterising weak interactions in solution. The challenge of detecting hydrogen and halogen bonds in particular, at low concentrations, has been addressed by means of the development of a new NMR spectroscopic methodology, while the current state of the art has been used to disprove the existence of a recently proposed new cation-cation interaction in solution.

Papers I-II describe the development of a new NMR methodology that makes use of paramagnetism-affected NMR observables to allow the detection and characterisation of weak interaction forces in dilute solutions, under conditions that would not allow their characterisation with the current techniques.

Paper I explores the new paramagnetic NMR technique by attachment of a Lewis base to a paramagnetic lanthanide complex, to study Lewis base- Lewis acid interactions. Detection of transferred pseudocontact shifts, residual dipolar couplings and paramagnetic relaxation enhancement on the diamagnetic interaction partner validated the concept. Evaluation of the interaction of a series of hydrogen and halogen bond donors of varying strength indicated that interactions as weak as $K_a = 0.6$ M^{-1} are detectable at 1.82 mM concentration, whereas interactions as weak as $K_a = 2.4$ M^{-1} can be characterised in solution in terms of association constant using this novel technique. Weak interactions can thus be detected in solutions at least 6 times more dilute than those characterisable to date with standard techniques[55]–the actual number being much higher in cases where weaker HB's were studied.

Paper II complements Paper I by demonstrating that the concept works independent of whether the donor or acceptor has been tagged paramagnetically. Investigating the interaction of a paramagnetically-tagged halogen bond donor with two Lewis bases in acetonitrile solution indicated that interactions possessing $K_a = 2.29$ M^{-1} can be characterised at a 2.20 mM concentration of host lanthanide tag. This is at least a ten times lower concentration than that has been previously possible. PRE, PCS's and RDC's, combined, allowed the detailed characterisation of the geometry of the halogen bond complex. This is astounding as the 3D structure determination of non-covalent complexes in solution is a great challenge for current spectroscopic techniques.

Paper III uses well-established solution NMR techniques to re-evaluate the existence of the recently proposed nucleophilic iodonium interaction (NII) in solution. Using [bis(4-methylpyridine)silver(I)]$^+$ and [bis(4-methylpyridine)iodine(I)]$^+$ complexes as model systems, ^{1}H,^{15}N HMBC and DOSY analysis were used to reveal the absence of attractive forces between iodine(I) and silver(I) in solution. The originally reported NMR observations were explained by their moisture induced decomposition, leading to chemical shift changes due to chemical exchange. DFT studies supported these conclusions by suggesting that the interaction is too weak to be detectable in solution, and that the weak attractive force, undetectable yet predictable computationally, does not originate from a charge transfer from iodine(I) to silver(I).

Overall, this thesis indicates the need for the critical evaluation of spectroscopic data. By providing a proof of concept, it also paves the way for the development of a new paramagnetic NMR technique that not only allows the determination of association constants at much lower concentrations than has ever been possible, but also allows the determination of the 3D structure of weak non-covalent complexes in solution; the latter is unprecedented. It allows one to essentially see the interaction of two weakly bound partners in solution to some degree–something only achievable in the solid state to date. These paramagnetism-affected observables are not dependent on the type of interaction, and require only a small fraction of bound complex to be of use. It appears likely that the studies described herein will represent the first of many investigations to make use of this strategy, where solvent effects, competition experiments and many other types of weak binding can be probed in the future.

7. Sammanfattning på Svenska

Molekyler interagerar med varandra genom svaga bindningar, vilka oftast kallas för "intermolekylära" krafter. Denna typ av interaktion återfinns i ett brett spektrum av styrkor och är av stor betydelse för hur vår värld fungerar. Att mäta intermolekylära interaktioner är dock fortfarande utmanande i lösningar, detta eftersom lösningsmedlet stör och tampas med de svaga interaktionerna vilket skapar obalans i lösningen.

Vätebindning är en typ av svag interaktion som ger vattnet dess egenskaper, DNA dess dubbelhelix, och möjliggör även för viktiga biokemiska processer. I alla dessa exempel är svaga vätebindningar temporärt formade vid låga koncentrationer, vilka oftast är mycket svåra att studera.

Ytterligare en svag interaktion, vars karaktär till stora delar liknar vätebindningar, kallas för halogenbindning. Interaktionen väntas spela en stor roll i nya läkemedels selektivitet och affinitet och kan användas för att styra egenskaperna hos avancerat material. Studierna kring halogenbindning är mycket begränsade, hittills har de mest studerats i kristaller och genom beräkningar. Förståelsen av halogenbindningarnas egenskaper i lösning släpar dock efter, detta då halogenbindningar är för svaga för att upptäckas och karaktäriseras i lösning med nuvarande teknik.

Mot bakgrund av detta har vi utvecklat ett helt nytt tillvägagångssätt för att upptäcka och kvantifiera halogenbindning i mycket små mängder.

Vi skapade nya molekyler som kapslar in lantanidmetalljoner. Dessa är paramagnetiska på grund av att de har fria elektroner och har ursprungligen upptäckts i Ytterby. Molekylerna användes därefter för att skapa vätebindningar till andra fria molekyler i lösningar. När vi placerade utspädda blandningar av de två i ett starkt magnetfält, kunde vi genom kärnmagnetisk resonansspektroskopi (NMR) se samspelet mellan molekylerna. Detta är första gången ett samspel mellan molekyler som interagerar så svagt kunde detekteras i utspädd lösning.

Genom att systematiskt addera den ena molekylen till den andra i små mängder (s.k. titrering), kunde vi mäta dem hittills svårstuderade paramagnetiska

NMR-effekterna. Styrkan i interaktionen och orienteringen av interaktions-parterna kunde bestämmas. Detta saknar motstycke. För att säkerställa en robust och tillförlitlig mätning, testade vi tre olika starka vätebindningsinteraktioner, samt gjorde en rad referensmätningar.

Vi använde sedan denna metodik till att studera halogenbindning i lösning. Samma koncept som ovan användes för att undersöka svaga kemiska bindningar så att antingen den ena eller den andra interaktionspartnern var kopplad till ett lantanidkomplex. Studien visade att även halogenbindningar kan kvantifieras med denna metod. Mätningarna möjliggjorde bestämningen av 3D-strukturen för molekylära komplex i utspädd lösning, på ett sätt som tidigare endast varit möjligt för fasta prover. Vi valde att studera halogenbindningar eftersom deras egenskaper ännu inte är välförstådda och en ökad förståelse skulle hjälpa deras rationella användning i läkemedelsdesign. Idag är över en tredjedel av befintligt läkemedel halogenerat och antalet halogenerade läkemedel ökar år efter år.

Sammanfattningsvis kan denna teknik tillåta en att se svaga bindningsfenomen vid mycket, mycket lägre koncentrationer, än vad som tidigare var möjligt!

Denna nyutvecklade NMR-metodiken som presenteras här förväntas vara användbar för studier av alla typer av kemiska interaktionskrafter, samt bistå med svar på flertalet olika vetenskapliga utmaningar som för närvarande inte kan besvaras med dem existerande metoder. Hittills har ingen kunnat studera så svaga interaktioner vid så låga koncentrationer. Vår teknik har stor potential att förändra hur vi analyserar molekylernas interaktion sinsemellan.

När det gäller halogenbindning undersökte vi även en ny typ av interaktion, som kallas "nukleofil jodoniuminteraktion" (NII) mellan jod(I)- och silver(I)-komplex. Denna nyss föreslagna interaktionen studerades med NMR i lösning. Vi kunde inte se några tecken på interaktion mellan de två molekylerna med avancerade NMR experiment. Genom att kontaminera enskilda prover och blandningar med spår av vatten, undersökte vi ifall partiell provnedbrytning kunde förklara de ursprungligen rapporterade observationerna. Så var fallet. Vi bevisade att den ursprungliga rapporten av interaktionen mellan jod(I)- och silver(I)-komplex, grundade sig på feltolkning av data från delvis nedbrutna kontaminerade (blöta) prover. Beräkningar visade att även om den föreslagna interaktionen existerade, skulle den vara för svag för att upptäckas i lösning, vilket bekräftar att rapporten om "nukleofil jodoniuminteraktion" (NII) baserar sig på felaktig datatolkning. Den lärdom vi drar av detta är att ifrågasätta resultat som inte verkar rimliga. Är det för bra för att vara sant så är det troligen fel.

8. Acknowledgements

I would first like to thank anyone who has read this far. I hope that it's been a fairly enjoyable experience to flick through the pages of this thesis ☺.

Mate, thanks for everything. For all the help and support. For all the endless days and nights put into these projects. For all of the scientific discussions together and for imparting even a fraction of your wisdom upon me. For your encouragement and for all your optimism. For your perseverance, especially in the years when things didn't look to be going my way. For all the moral support and the life advice. For the countless bike rides and weekend fika stops. For creating a comfortable work environment that I'll surely miss. I really couldn't have asked for more from a supervisor.

Rui, you were my go-to-guy for most things in and around the lab. For that, I'm so grateful. It's been a tough journey together throughout the years and it's been a pleasure to work with you and discuss everything we have. I hope that there's still space in your head for all of the fresh NMR knowledge now being thrown at you.

Bea, thanks for being so fun to work alongside. Your cheerfulness, light-hearted complaints and tiny coffees were a treat. And it's great to see that BBBcrap has been used to study halogen bonding–maybe now you are convinced that"卤素键不存在" isn't true after all…

The Paramagnetic Subgroup, further featuring: Pieterje, Mau, René, Daniel vdH, Edward, Mateo and Anna; thanks for all of the collaboration, the useful ideas and the many, many attempts to get these projects working. It would have been a struggle to succeed without all of your contributions.

The Erdelyi Group, both past and present. Much alike the heroes above, you have been integral in making this project work out. Thanks for this and for all of the time spent in meetings troubleshooting my problems and presentations.

Thanks, Adolf, for your support as my co-supervisor and for all your help with NMR. Thanks, Helena G., for looking out for me and for pushing me to this

point. Thanks, Jan K., for your help and support when starting here, and to all the other PI's around the department for your constant support.

Thanks to all that make the department work as well as it does. To Helena Danielsson for being so pragmatic during the pandemic. To Gunnar, Farshid, Johanna A. and co. for all the help in keeping things up and running. To Francoise for your kindness and all of the help with teaching. And to all in admin and behind the scenes for allowing me to focus on my research.

Thanks to the various sources of funding: Åforsk (Travel Grant), Apotekarsocieteten (2 × IF:s stiftelse), UU (Liljewalchs Resestip) and Smålands Nation (Anna Maria Lundins Travel Grant), that have allowed me to attend numerous courses and conferences during the course of my PhD.

Thanks in particular to Stefan, Fabio, Jacob, Michael and Chris for the many adventures and tinnies had over the years! And to: Mau & Hermina, Marie, Kate & Daniel, Carina, Kate & Jakub, Fredric, Matic & Kilian, Ivan, Bart, Filip, Nich and Wills for all the good times and much needed distractions! And to all of the colleagues met over the years here at BMC for all of your help and overall good chat that kept me going.

Thanks Mum, Dad, Jessica, Granny Betty and family. I wouldn't have gotten this far without your encouragement over this past decade or so spent in higher education. If anyone asks what I'm actually doing, you're safest just to say 'science.'"

And lastly, to Mariya. Thanks. I doubt that you're aware of how much you support me in everything, so here's a small hint that you can have in print.

Cheers.

References

[1]   C. A. Coulson, *Inaugural Lecture: Oxford University 26 Oct,* **1952**.
[2]   P. Ball, *Nature* **2011**, *469*, 26-28.
[3]   K. Goldsby, R. Chang, McGraw-Hill Education, **2015**.
[4]   L. Turunen, M. Erdélyi, *Chemical Society Reviews* **2020**, *49*, 2688-2700.
[5]   C. B. Aakeroy, D. L. Bryce, G. R. Desiraju, A. Frontera, A. C. Legon, F. Nico-tra, K. Rissanen, S. Scheiner, G. Terraneo, P. Metrangolo, *Pure and Applied Chemistry* **2019**, *91*, 1889-1892.
[6]   D. Bryce, G. Desiraju, A. Frontera, A. Legon, F. Nicotra, K. Rissanen, S. Sche-iner, G. Terraneo, P. Metrangolo, G. Resnati, *IUPAC project* **2016**, 001-002.
[7]   J. S. Ward, A. Frontera, K. Rissanen, *Chemical Communications* **2021**, *57*, 5094-5097.
[8]   J. S. Ward, A. Frontera, K. Rissanen, *Inorganic chemistry* **2021**, *60*, 5383-5390.
[9]   L. Pauling, C. University, C. U. Press, *The Nature of the Chemical Bond and the Structure of Molecules and Crystals: An Introduction to Modern Structural Chemistry*, Cornell University Press, **1960**.
[10] R. H. Crabtree, *Chemical Society Reviews* **2017**, *46*, 1720-1729.
[11] M. S. Silberberg, P. Amateis, R. Venkateswaran, L. Chen, *Chemistry: The molecular nature of matter and change*, Mosby St. Louis, MO, **1996**.
[12] M. G. Sarwar, B. Dragisic, L. J. Salsberg, C. Gouliaras, M. S. Taylor, *J Am Chem Soc* **2010**, *132*, 1646-1653.
[13] W. M. Latimer, W. H. Rodebush, *Journal of the American Chemical Society* **1920**, *42*, 1419-1433.
[14] L. Pauling, *Journal of the American Chemical Society* **1935**, *57*, 2680-2684.
[15] L. Pauling, Cornell University Press. Ithaca, NY, **1939**.
[16] G. C. Pimentel, A. L. McClellan, A. L. MacClellan, *The hydrogen bond*, WH freeman, **1960**.
[17] E. Arunan, G. R. Desiraju, R. A. Klein, J. Sadlej, S. Scheiner, I. Alkorta, D. C. Clary, R. H. Crabtree, J. J. Dannenberg, P. Hobza, H. G. Kjaergaard, A. C. Legon, B. Mennucci, D. J. Nesbitt, *Pure and Applied Chemistry* **2011**, *83*, 1637-1641.
[18] A. Buckingham, *Theoretical treatments of hydrogen bonding* **1997**, 1-12.
[19] G. Gilli, P. Gilli, *The nature of the hydrogen bond: outline of a comprehensive hydrogen bond theory, Vol. 23*, Oxford university press, **2009**.
[20] Y. Gu, T. Kar, S. Scheiner, *Journal of the American Chemical Society* **1999**, *121*, 9411-9422.
[21] M. Nishio, *Physical Chemistry Chemical Physics* **2011**, *13*, 13873-13900.
[22] G. R. Desiraju, T. Steiner, *The weak hydrogen bond: in structural chemistry and biology, Vol. 9*, International Union of Crystal, **2001**.
[23] D. Herschlag, M. M. Pinney, *Biochemistry* **2018**, *57*, 3338-3352.
[24] J. J. Colin, H. Gaultier de Claubry, *Ann. Chim* **1814**, *90*, 87-100.
[25] M. Colin, *Ann. Chim* **1814**, *91*, 252-272.

[26]   F. Guthrie, *Journal of the Chemical Society* **1863**, *16*, 239-244.
[27]   R. S. Mulliken, *Journal of the American Chemical Society* **1950**, *72*, 600-608.
[28]   R. S. Mulliken, *Journal of the American Chemical Society* **1952**, *74*, 811-824.
[29]   R. S. Mulliken, *The Journal of Physical Chemistry* **1952**, *56*, 801-822.
[30]   L. Turunen, J. H. Hansen, M. Erdélyi, *The Chemical Record* **2021**, *21*, 1252-1257.
[31]   O. Hassel, J. Hvoslef*, Vol. 8*, MUNKSGAARD INT PUBL LTD 35 NORRE SOGADE, PO BOX 2148, DK-1016 COPENHAGEN …, **1954**, pp. 873-873.
[32]   O. Hassel, C. Rømming, *Quarterly Reviews, Chemical Society* **1962**, *16*, 1-18.
[33]   O. Hassel, K. Stromme*, Vol. 12*, MUNKSGAARD INT PUBL LTD 35 NORRE SOGADE, PO BOX 2148, DK-1016 COPENHAGEN …, **1958**, pp. 1146-1147.
[34]   O. Hassel, K. Stromme, *Acta Chemica Scandinavica* **1959**, *13*, 1781-1786.
[35]   G. R. Desiraju, P. S. Ho, L. Kloo, A. C. Legon, R. Marquardt, P. Metrangolo, P. Politzer, G. Resnati, K. Rissanen, *Pure Appl. Chem* **2013**, *85*, 1711-1713.
[36]   P. Muller, *Pure and Applied Chemistry* **1994**, *66*, 1077.
[37]   A. Karpfen, in *Halogen Bonding: Fundamentals and Applications* (Eds.: P. Metrangolo, G. Resnati), Springer Berlin Heidelberg, Berlin, Heidelberg, **2008**, pp. 1-15.
[38]   G. Cavallo, P. Metrangolo, R. Milani, T. Pilati, A. Priimagi, G. Resnati, G. Terraneo, *Chem Rev* **2016**, *116*, 2478-2601.
[39]   D. A. Decato, E. A. John, O. B. Berryman, in *Halogen Bonding in Solution*, **2021**, pp. 1-41.
[40]   T. Brinck, J. S. Murray, P. Politzer, *International Journal of Quantum Chemistry* **1992**, *44*, 57-64.
[41]   P. Politzer, P. Lane, M. C. Concha, Y. Ma, J. S. Murray, *Journal of Molecular Modeling* **2007**, *13*, 305-311.
[42]   H. A. Bent, *Chemical Reviews* **1968**, *68*, 587-648.
[43]   C. Wang, D. Danovich, Y. Mo, S. Shaik, *Journal of Chemical Theory and Computation* **2014**, *10*, 3726-3737.
[44]   P. Politzer, J. S. Murray, T. Clark, *Journal of Molecular Modeling* **2015**, *21*, 52.
[45]   T. Clark, M. Hennemann, J. S. Murray, P. Politzer, *Journal of molecular modeling* **2007**, *13*, 291-296.
[46]   Y. Zhang, B. Ji, A. Tian, W. Wang, *J Chem Phys* **2012**, *136*, 141101.
[47]   N. Schulz, P. Sokkar, E. Engelage, S. Schindler, M. Erdelyi, E. Sanchez-Garcia, S. M. Huber, *Chemistry - A European Journal* **2018**, *24*, 3464-3473.
[48]   P. Metrangolo, H. Neukirch, T. Pilati, G. Resnati, *Accounts of chemical research* **2005**, *38*, 386-395.
[49]   A. Karim, M. Reitti, A.-C. C. Carlsson, J. Gräfenstein, M. Erdélyi, *Chem. Sci.* **2014**, *5*, 3226-3233.
[50]   A. C. Carlsson, J. Grafenstein, J. L. Laurila, J. Bergquist, M. Erdelyi, *Chem Commun (Camb)* **2012**, *48*, 1458-1460.
[51]   S. M. Huber, J. D. Scanlon, E. Jimenez-Izal, J. M. Ugalde, I. Infante, *Physical Chemistry Chemical Physics* **2013**, *15*, 10350-10357.
[52]   L. C. Gilday, S. W. Robinson, T. A. Barendt, M. J. Langton, B. R. Mullaney, P. D. Beer, *Chemical Reviews* **2015**, *115*, 7118-7195.
[53]   A. V. Jentzsch, D. Emery, J. Mareda, S. K. Nayak, P. Metrangolo, G. Resnati, N. Sakai, S. Matile, *Nature Communications* **2012**, *3*, 905.
[54]   C. C. Robertson, R. N. Perutz, L. Brammer, C. A. Hunter, *Chemical Science* **2014**, *5*, 4179-4183.

[55] C. C. Robertson, J. S. Wright, E. J. Carrington, R. N. Perutz, C. A. Hunter, L. Brammer, *Chem Sci* **2017**, *8*, 5392-5398.

[56] A. Vargas Jentzsch, *Pure and Applied Chemistry* **2015**, *87*, 15-41.

[57] P. S. Ho, in *Halogen Bonding I: Impact on Materials Chemistry and Life Sciences* (Eds.: P. Metrangolo, G. Resnati), Springer International Publishing, Cham, **2015**, pp. 241-276.

[58] B. Watson, O. Grounds, W. Borley, S. V. Rosokha, *Phys Chem Chem Phys* **2018**, *20*, 21999-22007.

[59] C. C. Robertson, R. N. Perutz, L. Brammer, C. A. Hunter, *Chem. Sci.* **2014**, *5*, 4179-4183.

[60] M. T. Messina, P. Metrangolo, W. Navarrini, S. Radice, G. Resnati, G. Zerbi, *Journal of Molecular Structure* **2000**, *524*, 87-94.

[61] L. K. Mork, V. Tat, D. J. Ulness, B. G. Erickson, M. W. Gealy, *Journal of Molecular Liquids* **2018**, *271*, 647-654.

[62] M. T. Messina, P. Metrangolo, W. Panzeri, E. Ragg, G. Resnati, *Tetrahedron Letters* **1998**, *39*, 9069-9072.

[63] P. Metrangolo, W. Panzeri, F. Recupero, G. Resnati, *Journal of Fluorine Chemistry* **2002**, *114*, 27-33.

[64] R. Cabot, C. A. Hunter, *Chem Commun (Camb)* **2009**, 2005-2007.

[65] X. Pang, W. J. Jin, *New Journal of Chemistry* **2015**, *39*, 5477-5483.

[66] C. Cavallotti, P. Metrangolo, F. Meyer, F. Recupero, G. Resnati, *J Phys Chem A* **2008**, *112*, 9911-9918.

[67] L. Gualandi, E. Mezzina, P. Franchi, M. Lucarini, *Chemistry* **2016**, *22*, 16017-16021.

[68] C. Zhao, Y. Lu, Z. Zhu, H. Liu, *J Phys Chem A* **2018**, *122*, 5058-5068.

[69] D. von der Heiden, A. Vanderkooy, M. Erdélyi, *Coordination Chemistry Reviews* **2020**, *407*.

[70] N. Schulz, S. Schindler, S. M. Huber, M. Erdelyi, *J Org Chem* **2018**, *83*, 10881-10886.

[71] M. R. J. F. Bertrán, *Organic Magnetic Resonance* **1979**, *12*, 92-94.

[72] Y. Z. Zheng, N. N. Wang, Y. Zhou, Z. W. Yu, *Phys Chem Chem Phys* **2014**, *16*, 6946-6956.

[73] O. Dumele, D. Wu, N. Trapp, N. Goroff, F. Diederich, *Org Lett* **2014**, *16*, 4722-4725.

[74] S. L. Cockroft, C. A. Hunter, *Chem Soc Rev* **2007**, *36*, 172-188.

[75] P. D. Rege, O. L. Malkina, N. S. Goroff, *J Am Chem Soc* **2002**, *124*, 370-371.

[76] J. A. Webb, J. E. Klijn, P. A. Hill, J. L. Bennett, N. S. Goroff, *J Org Chem* **2004**, *69*, 660-664.

[77] H. Andersson, A.-C. C. Carlsson, B. Nekoueishahraki, U. Brath, M. Erdélyi, **2015**, pp. 73-210.

[78] S. B. Hakkert, J. Grafenstein, M. Erdelyi, *Faraday Discuss* **2017**, *203*, 333-346.

[79] S. Castro-Fernández, I. R. Lahoz, A. L. Llamas-Saiz, J. L. Alonso-Gómez, M.-M. Cid, A. Navarro-Vázquez, *Organic Letters* **2014**, *16*, 1136-1139.

[80] A. C. Carlsson, K. Mehmeti, M. Uhrbom, A. Karim, M. Bedin, R. Puttreddy, R. Kleinmaier, A. A. Neverov, B. Nekoueishahraki, J. Grafenstein, K. Rissanen, M. Erdelyi, *J Am Chem Soc* **2016**, *138*, 9853-9863.

[81] A.-C. C. Carlsson, M. Uhrbom, A. Karim, U. Brath, J. Gräfenstein, M. Erdélyi, *CrystEngComm* **2013**, *15*.

[82] A. C. Carlsson, A. X. Veiga, M. Erdelyi, *Halogen Bonding II: Impact on Materials Chemistry and Life Sciences, Vol. 358*, Springer, **2015**.

[83] L. Fielding, *Tetrahedron* **2000**, *34*, 6151-6170.

[84]   P. Job, *Ann. chim* **1928**, *9*.

[85]   D. Brynn Hibbert, P. Thordarson, *Chem Commun (Camb)* **2016**, *52*, 12792-12805.

[86]   M. G. Sarwar, B. Dragisic, S. Sagoo, M. S. Taylor, *Angew Chem Int Ed Engl* **2010**, *49*, 1674-1677.

[87]   E. Dimitrijevic, O. Kvak, M. S. Taylor, *Chem Commun (Camb)* **2010**, *46*, 9025-9027.

[88]   E. L. Hahn, *Physical Review* **1950**, *80*, 580-594.

[89]   E. O. Stejskal, J. E. Tanner, *The Journal of Chemical Physics* **1965**, *42*, 288-292.

[90]   A. Mix, J.-H. Lamm, J. Schwabedissen, E. Gebel, H.-G. Stammler, N. W. Mitzel, *Chemical Communications* **2022**, *58*, 3465-3468.

[91]   G. Ciancaleoni, A. Macchioni, L. Rocchigiani, C. Zuccaccia, *RSC Advances* **2016**, *6*, 80604-80612.

[92]   T. M. Beale, M. G. Chudzinski, M. G. Sarwar, M. S. Taylor, *Chem Soc Rev* **2013**, *42*, 1667-1680.

[93]   S. Wilcox, W. Herrebout, M. Erdelyi, *Halogen Bonding in Solution* **2021**, 153-194.

[94]   R. A. Thorson, G. R. Woller, Z. L. Driscoll, B. E. Geiger, C. A. Moss, A. L. Schlapper, E. D. Speetzen, E. Bosch, M. Erdélyi, N. P. Bowling, *European Journal of Organic Chemistry* **2015**, *2015*, 1685-1695.

[95]   P. E. Hansen, J. Spanget-Larsen, *Molecules* **2017**, *22*, 552.

[96]   S. H. Jungbauer, D. Bulfield, F. Kniep, C. W. Lehmann, E. Herdtweck, S. M. Huber, *J Am Chem Soc* **2014**, *136*, 16740-16743.

[97]   G. Cooke, V. M. Rotello, *Chemical Society Reviews* **2002**, *31*, 275-286.

[98]   J. L. Cook, C. A. Hunter, C. M. R. Low, A. Perez-Velasco, J. G. Vinter, *Angewandte Chemie International Edition* **2007**, *46*, 3706-3709.

[99]   K. Hirose, *Journal of inclusion phenomena and macrocyclic chemistry* **2001**, *39*, 193-209.

[100] P. Thordarson, *Chemical Society Reviews* **2011**, *40*, 1305-1323.

[101] J. F. Bertrán, M. Rodríguez, *Organic Magnetic Resonance* **1979**, *12*, 92-94.

[102] Q. Miao, C. Nitsche, H. Orton, M. Overhand, G. Otting, M. Ubbink, *Chemical Reviews* **2022**, *122*, 9571-9642.

[103] C. Nitsche, G. Otting, *Progress in Nuclear Magnetic Resonance Spectroscopy* **2017**, *98-99*, 20-49.

[104] M. Allegrozzi, I. Bertini, M. B. L. Janik, Y.-M. Lee, G. Liu, C. Luchinat, *Journal of the American Chemical Society* **2000**, *122*, 4154-4161.

[105] G. Parigi, C. Luchinat, in *Paramagnetism in Experimental Biomolecular NMR*, The Royal Society of Chemistry, **2018**, pp. 1-41.

[106] I. Bertini, C. Luchinat, G. Parigi, E. Ravera, *NMR of paramagnetic molecules: applications to metallobiomolecules and models*, Elsevier, **2016**.

[107] C. A. Softley, M. J. Bostock, G. M. Popowicz, M. Sattler, *Journal of Biomolecular NMR* **2020**, *74*, 287-309.

[108] T. Müntener, D. Joss, D. Häussinger, S. Hiller, *Chemical Reviews* **2022**, *122*, 9422-9467.

[109] H. M. McConnell, R. E. Robertson, *The Journal of Chemical Physics* **1958**, *29*, 1361-1365.

[110] G. Pintacuda, M. John, X.-C. Su, G. Otting, *Accounts of Chemical Research* **2007**, *40*, 206-212.

[111] X.-C. Su, K. McAndrew, T. Huber, G. Otting, *Journal of the American Chemical Society* **2008**, *130*, 1681-1687.

[112] I. Bertini, C. Luchinat, G. Parigi, *Concepts in Magnetic Resonance* **2002**, *14*, 259-286.

[113] K. Chen, N. Tjandra, in *NMR of Proteins and Small Biomolecules* (Ed.: G. Zhu), Springer Berlin Heidelberg, Berlin, Heidelberg, **2012**, pp. 47-67.

[114] M. Blackledge, *Progress in Nuclear Magnetic Resonance Spectroscopy* **2005**, *46*, 23-61.

[115] A. Navarro-Vázquez, *Magnetic Resonance in Chemistry* **2012**, *50*, S73-S79.

[116] Y. Liu, A. Navarro-Vázquez, R. R. Gil, C. Griesinger, G. E. Martin, R. T. Williamson, *Nature Protocols* **2019**, *14*, 217-247.

[117] X.-C. Su, G. Otting, *Journal of biomolecular NMR* **2010**, *46*, 101-112.

[118] H. W. Orton, T. Huber, G. Otting, *Magn. Reson.* **2020**, *1*, 1-12.

[119] W. Jahnke, *ChemBioChem* **2002**, *3*, 167-173.

[120] G. Otting, *Annual Review of Biophysics* **2010**, *39*, 387-405.

[121] G. Pintacuda, M. John, X. C. Su, G. Otting, *Acc Chem Res* **2007**, *40*, 206-212.

[122] M. Allegrozzi, I. Bertini, M. B. Janik, Y.-M. Lee, G. Liu, C. Luchinat, *Journal of the American Chemical Society* **2000**, *122*, 4154-4161.

[123] M. Bottrill, L. Kwok, N. J. Long, *Chemical Society Reviews* **2006**, *35*, 557-571.

[124] N. C. Martinez-Gomez, H. N. Vu, E. Skovran, *Inorganic Chemistry* **2016**, *55*, 10083-10089.

[125] Y. W. Ebright, Y. Chen, P. S. Pendergrast, R. H. Ebright, *Biochemistry* **1992**, *31*, 10664-10670.

[126] M. Prudencio, J. Rohovec, J. A. Peters, E. Tocheva, M. J. Boulanger, M. E. Murphy, H. J. Hupkes, W. Kosters, A. Impagliazzo, M. Ubbink, *Chemistry–A European Journal* **2004**, *10*, 3252-3260.

[127] J. T. Brewster, G. D. Thiabaud, P. Harvey, H. Zafar, J. F. Reuther, S. Dell'Acqua, R. M. Johnson, H. D. Root, P. Metola, A. Jasanoff, L. Casella, J. L. Sessler, *Chem* **2020**, *6*, 703-724.

[128] I. Bertini, M. B. L. Janik, Y.-M. Lee, C. Luchinat, A. Rosato, *Journal of the American Chemical Society* **2001**, *123*, 4181-4188.

[129] D. Parker, E. A. Suturina, I. Kuprov, N. F. Chilton, *Accounts of Chemical Research* **2020**, *53*, 1520-1534.

[130] G. Pintacuda, G. Otting, *Journal of the American Chemical Society* **2002**, *124*, 372-373.

[131] Z. Gong, C. D. Schwieters, C. Tang, *Methods* **2018**, *148*, 48-56.

[132] T. J. Clough, L. Jiang, K. L. Wong, N. J. Long, *Nat Commun* **2019**, *10*, 1420.

[133] P. Caravan, J. J. Ellison, T. J. McMurry, R. B. Lauffer, *Chemical Reviews* **1999**, *99*, 2293-2352.

[134] M. A. S. Hass, M. Ubbink, *Current Opinion in Structural Biology* **2014**, *24*, 45-53.

[135] G. Otting, *Annu Rev Biophys* **2010**, *39*, 387-405.

[136] M. Erdélyi, E. d'Auvergne, A. Navarro-Vázquez, A. Leonov, C. Griesinger, *Chemistry – A European Journal* **2011**, *17*, 9368-9376.

[137] U. Brath, S. I. Swamy, A. X. Veiga, C. C. Tung, F. Van Petegem, M. Erdelyi, *J Am Chem Soc* **2015**, *137*, 11391-11398.

[138] A. Fallek, M. Portnoy, *ChemistrySelect* **2019**, *4*, 3175-3179.

[139] J. H. S. K. Monteiro, D. Machado, L. M. de Hollanda, M. Lancellotti, F. A. Sigoli, A. de Bettencourt-Dias, *Chemical Communications* **2017**, *53*, 11818-11821.

[140] E. R. Neil, M. A. Fox, R. Pal, L.-O. Pålsson, B. A. O'Sullivan, D. Parker, *Dalton Transactions* **2015**, *44*, 14937-14951.

[141] K. Mason, A. C. Harnden, C. W. Patrick, A. W. J. Poh, A. S. Batsanov, E. A. Suturina, M. Vonci, E. J. L. McInnes, N. F. Chilton, D. Parker, *Chemical Communications* **2018**, *54*, 8486-8489.

[142] C. P. Butts, C. R. Jones, J. N. Harvey, *Chemical Communications* **2011**, *47*, 1193-1195.

[143] R. Dass, P. Kasprzak, W. Koźmiński, K. Kazimierczuk, *Journal of Magnetic Resonance* **2016**, *265*, 108-116.

[144] L. H. Wieske, M. Erdélyi, *Magnetic Resonance in Chemistry* **2021**, *59*, 723-737.

[145] J. D. Phillipson, N. G. Bisset, *Phytochemistry* **1972**, *11*, 2547-2553.

[146] J. S. Ward, A. Frontera, K. Rissanen, *Chemical Communications* **2022**, *58*, 5041-5041.

[147] S. Yu, P. Kumar, J. S. Ward, A. Frontera, K. Rissanen, *Chem* **2021**, *7*, 948-958.

[148] G. T. Cochran, J. F. Allen, N. P. Marullo, *Inorganica Chimica Acta* **1967**, *1*, 109-112.

[149] S. M. Soliman, Y. N. Mabkhot, A. Barakat, H. A. Ghabbour, *Journal of Coordination Chemistry* **2017**, *70*, 1339-1356.

[150] S. Lindblad, F. B. Németh, T. Földes, A. Vanderkooy, I. Pápai, M. Erdélyi, *Chemical Communications* **2020**, *56*, 9671-9674.

[151] J. Barluenga, *Pure and applied chemistry* **1999**, *71*, 431-436.

[152] R. Zingaro, W. Witmer, G. Kauffman, K. Stevens, *INORGANIC SYNTHESES* **1963**, *7*, 169-176.

[153] A. C. Carlsson, J. Grafenstein, A. Budnjo, J. L. Laurila, J. Bergquist, A. Karim, R. Kleinmaier, U. Brath, M. Erdelyi, *J Am Chem Soc* **2012**, *134*, 5706-5715.

[154] D. von der Heiden, K. Rissanen, M. Erdélyi, *Chemical Communications* **2020**, *56*, 14431-14434.

[155] D. Sethio, G. Raggi, R. Lindh, M. Erdélyi, *Journal of Chemical Theory and Computation* **2020**, *16*, 7690-7701.

[156] A. Vanderkooy, A. K. Gupta, T. Foldes, S. Lindblad, A. Orthaber, I. Papai, M. Erdelyi, *Angew Chem Int Ed Engl* **2019**, *58*, 9012-9016.

Acta Universitatis Upsaliensis

Digital Comprehensive Summaries of Uppsala Dissertations
from the Faculty of Science and Technology 2184

Editor: The Dean of the Faculty of Science and Technology